Polytechnic Institute of New York

Department of Aerospace Engineering and Applied Mechanics

12

FC

WIND TUNNEL EXPERIMENTS ON WAKES IN STRATIFIED FLOW INCLUDING MODELING CRITERIA AND DEVELOPMENT OF EXPERIMENTAL EQUIPMENT

by

Gordon H. Strom

This research was supported by the Advanced Research Projects Agency of the Department of Defense and was monitored by the Office of Naval Research under Contract No. N00014-67-A-0438-0017

POLYTECHNIC INSTITUTE OF NEW YORK

AERODYNAMICS LABORATORIES

June 1976

POLY-AE/AM Report No. 76-11

Unclassified

SECURITY CLASSIFICATION OF THIS PAGE (When Data Entered)

REPORT DOCUMENTATION PAGE

READ INSTRUCTIONS BEFORE COMPLETING FORM

(14) 1. REPORT NUMBER: POLY-AE/AM [redacted]-76-11

2. GOVT ACCESSION NO.

3. RECIPIENT'S CATALOG NUMBER: 1

(6) 4. TITLE (and Subtitle): WIND TUNNEL EXPERIMENTS ON WAKES IN STRATIFIED FLOW INCLUDING CRITERIA AND DEVELOPMENT OF EXPERIMENTAL EQUIPMENT. (modeling)

5. TYPE OF REPORT & PERIOD COVERED: Scientific - Interim rept.,

6. PERFORMING ORG. REPORT NUMBER

(10) 7. AUTHOR(s): Gordon H. Strom

(15) 8. CONTRACT OR GRANT NUMBER(s): N-00014-67-A-0438-0017, ARPA Order-2684

9. PERFORMING ORGANIZATION NAME AND ADDRESS
Polytechnic Institute of New York
~~Aerodynamics Laboratories~~
Route 110, Farmingdale, NY 11735

10. PROGRAM ELEMENT, PROJECT, TASK AREA & WORK UNIT NUMBERS: ARPA Order No. 2684

11. CONTROLLING OFFICE NAME AND ADDRESS
Advanced Research Projects Agency
1400 Wilson Blvd.
Arlington, VA 22209

(11) 12. REPORT DATE: Jun[redacted]76

13. NUMBER OF PAGES: 60

14. MONITORING AGENCY NAME & ADDRESS (if different from Controlling Office)
Office of Naval Research
Dept. of the Navy
Arlington, VA 22217

(12) 71 p.

15. SECURITY CLASS. (of this report): Unclassified

15a. DECLASSIFICATION/DOWNGRADING SCHEDULE

16. DISTRIBUTION STATEMENT (of this Report)
Approved for public release; distribution unlimited.

17. DISTRIBUTION STATEMENT (of the abstract entered in Block 20, if different from Report)

18. SUPPLEMENTARY NOTES

19. KEY WORDS (Continue on reverse side if necessary and identify by block number)
Scale model turbulent wakes
Stratified flow
Modeling criteria
Very low speed wind tunnel experimentation

20. ABSTRACT (Continue on reverse side if necessary and identify by block number)
Wind tunnel experiments were conducted on dimensions of the turbulent wake from an 8 inch disk model in thermally stratified flow. Results were interpreted in terms of densimetric Froude number as the modeling criterion. The substantial agreement with reported hydrodynamic experiments shows the potential for using wind tunnels to study submarine wakes in stratified flow. An additional modeling criterion for vertical density gradient based on momentum flux may be important for momentumless wakes. (over)

DD FORM 1 JAN 73 1473 EDITION OF 1 NOV 65 IS OBSOLETE

Unclassified

SECURITY CLASSIFICATION OF THIS PAGE (When Data Entered)

20. Abstract (Contd.)

Development of experimental equipment needed to obtain uniform wind tunnel airstreams at very low speeds with thermal stratification is described.

WIND TUNNEL EXPERIMENTS ON WAKES IN STRATIFIED FLOW INCLUDING MODELING CRITERIA AND DEVELOPMENT OF EXPERIMENTAL EQUIPMENT

by

Gordon H. Strom

This research was supported by the Advanced Research Projects Agency of the Department of Defense and was monitored by the Office of Naval Research under Contract No. N00014-67-A-0438-0017

POLYTECHNIC INSTITUTE OF NEW YORK

AERODYNAMICS LABORATORIES

June 1976

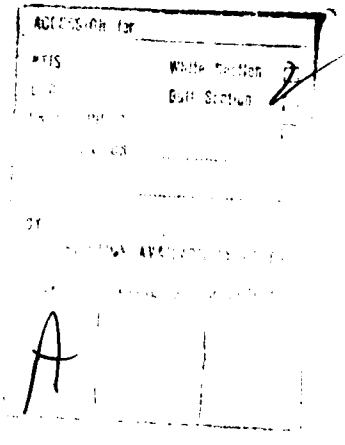

POLY-AE/AM Report No. 76-11

WIND TUNNEL EXPERIMENTS ON WAKES IN STRATIFIED FLOW INCLUDING MODELING CRITERIA AND DEVELOPMENT OF EXPERIMENTAL EQUIPMENT*

by

Gordon H. Strom**

Polytechnic Institute of New York
Aerodynamics Laboratories
Farmingdale, New York

ABSTRACT

Wind tunnel experiments were conducted on dimensions of the turbulent wake from an 8 inch disk model in thermally stratified flow. Results were interpreted in terms of densimetric Froude number as the modeling criterion. The substantial agreement with reported hydrodynamic experiments shows the potential for using wind tunnels to study submarine wakes in stratified flow. An additional modeling criterion for vertical density gradient based on momentum flux may be important for momentumless wakes. Development of experimental equipment needed to obtain uniform wind tunnel airstreams at very low speeds with thermal stratification is described.

---

*This research was supported by the Advanced Research Projects Agency of the Department of Defense and was monitored by the Office of Naval Research under Contract No. N00014-67-A-0438-0017.

**Professor of Aerospace Engineering

Contents

List of Figures

List of Figures (continued)

Symbols

A_a	propeller upstream tube cross-sectional area [Eq. (12)]
A_B	body frontal (cross-sectional) area [Eq. (20)]
A_p	propeller disk area [Eqs. (13), (14), and (17)]
A_w	propeller downstream tube cross-sectional area [Eq. (12)]
b_c	far wake horizontal width [Eq. (33), Fig. 3]
b_f	far wake vertical width [Eq. (36), Fig. 3]
b_h	intermediate wake horizontal width [Eq. (32), Fig. 3]
b_m	intermediate wake vertical width [Eq. (34), Fig. 3]
b_v	far wake vertical width [Eq. (35)]
b_∞	near wake horizontal and vertical width [Eq. (31), Fig. 3]
C_D	submarine body drag coefficient [Eq. (20]
C_t	propeller total thrust coefficient [Eq. (17)]
C_{te}	propeller local thrust coefficient for an element of flow [Eqs. (24) and (25)]
D	initial wake diameter in Reference 1 [Fig. 4]
D	fluid drag force on submarine body [Eq. (20)]
D_B	submarine body diameter [Fig. (1)]
D_B	model disk diameter
D_i	initial wake diameter [Fig. (1)]
D_p	propeller diameter
Fi	densimetric Froude number [Eq. (6)]
Fr	densimetric Froude number [Eq. (2)]
Fr′	velocity Froude number [Eq. (10)]

Symbols (continued)

g	acceleration due to gravity
L	submarine body length
m	subscript for model
P	Brunt-Vaisala time period [Eq. (3)]
p	subscript for prototype (full scale)
p	free stream fluid pressure
Δp	incremental increase in fluid pressure
Re	Reynolds number [Eq. (1)]
t	time [Eqs. (31-38), Fig. 4]
t	air temperature, ^{o}F [Figs. 11, 12, and 21]
T	propeller thrust force [Eqs. (14) and (17)]
T	absolute air temperature, ^{o}R [Eqs. (7b) and (47)]
u	free stream fluid speed relative to submarine or disk model, unstratified flow
u	free stream fluid speed relative to submarine or disk model at $z = 0$, stratified flow
$u(z)$	free stream fluid speed velative to submarine or disk model at elevation z
u_a	fluid speed near submarine [Eq. (12), Figs. 1 and 2]
u_p	fluid speed at propeller [Eq. (13), Fig. 2]
Δu_p	incremental increase in fluid speed at propeller [Eqs. (13) and (14), Fig. 2]
u_w	fluid speed in propeller slipstream [Eqs. (12) and (13), Figs. 1 and 2]
Δu_w	incremental increase in fluid speed in propeller slipstream [Eqs. (13) and (14), Fig. 2]
x	downstream distance relative to virtual origin [Figs. 1, 2, and 3]
x	downstream distance relative to heater section [Figs. 5 and 7]
x_M	downstream distance relative to disk model

Symbols (continued)

y	cross stream (horizontal) distance from disk model centerline
z	vertical distance from submarine or disk model centerline, positive downward [Figs. 1 and 2]
Γ	atmospheric adiabatic temperature gradient [Eq. (7b)]
θ	atmospheric potential temperature [Eqs. (7a) and (7b)]
λ	wave length [Eq. (4)]
μ	fluid dynamic viscosity
ν	fluid kinematic viscosity
ρ	fluid mass density, unstratified flow [Fig. 2]
ρ	fluid mass density at $z = 0$, stratified flow [Fig. 2]
$\rho(z)$	fluid mass density at elevation z, stratified flow [Fig. 2]

I. Introduction

Ocean water will under certain conditions have stably stratified density gradients in the vertical direction. These may be caused by vertical temperature gradients or by variation in salinity. The turbulent wake downstream of a submarine will under stable conditions be markedly different from that found with a neutral (zero) gradient. This may have important effects on submarine operation and on the surrounding flow field.

Results of many experimental programs employing scale model experiments are summarized in Reference 1. They show various features of wake growth and subsequent collapse. Following the initial wake growth, vertical wake thickness decreases and horizontal width increases. At greater downstream distances, thickness remains substantially constant while width continues to grow. These effects are caused by differences in fluid pressures inside and outside of the wake. Turbulent mixing in the wake partially eliminates the density gradient that exists in the surrounding undisturbed fluid.

An important aspect of scale model experimentation is the application of the appropriate scaling laws or modeling criteria. They determine the values that the test variables must have in a scale model experiment to accurately reproduce in miniature the characteristics of the prototype. Section II of this report is addressed to this subject. Merritt's study (Reference 1) employs a form of Froude number which relates model test velocity, size, and density gradient to those of the full scale counterpart. An additional criterion is developed in Section II from consideration of fluid forces produced by the submarine propeller. This further restricts the relations of model test variables. The experimental phase was not carried to the point of introducing propulsive forces, thus the significance of the additional criterion was not tested.

The bulk of past experimental programs used water as the fluid medium which is natural. One of the objectives of the present project is to determine the feasibility of using air as the fluid medium. An airstream with vertically varying temperature has a density gradient which can be used to represent a density gradient in water. The Environmental Wind Tunnel at Polytechnic has the capability of producing an airstream with controlled temperature gradients. With some modifications and additions to the existing wind tunnel, a successful series of experiments was conducted on the wake produced by a disk in stratified and neutral flow. Most of the reported hydrodynamic studies were made in specially constructed facilities and with relatively small models. A wind tunnel with its larger test section dimensions allows the use of larger models which are easier to construct and operate, especially if a propulsive unit is included. It does not have problems of sealing model components from intrusion of water. Model accessibility for adjustments and changes is better.

II. Experimental Problems and Modeling Criteria

Past theoretical and experimental investigations with stratified fluids have emphasized the more distant wake regions in which the details of submarine configuration are of lesser importance. The results of those investigations are difficult or impossible to apply to specific submarines. They are not related to specific configurations or even body diameter or length. It will be shown in the following paragraphs that the modeling criteria applicable to the distant wake regions may not be sufficient for, nor even the same as those for regions closer to the submarine body and propeller. This arises from the change in relative importance of various types of fluid forces at different locations.

A. Presentation of Modeling Criteria

There are three types of fluid forces which are potentially important in these applications. They are inertial, gravitational, and viscous. A

modeling criterion (or similarity criterion, or scale factor) represents the ratio of two types of forces expressed in terms of various experimental variables. Three criteria will be presented and discussed in this section. Their development will be given in later sections. In common with many types of experimental investigations with scale models, the various criteria lead to conflicting requirements for scale model test variables.

The well known Reynolds number results from the ratio of inertial to viscous forces. It is given in terms of experimental variables as follows:

$$\text{Reynolds number} \quad Re = \rho \frac{u D_B}{\mu}$$

$$= \frac{u D_B}{\nu} \tag{1}$$

where ρ is fluid mass density, μ is dynamic viscosity, and ν is kinematic viscosity ($=\mu/\rho$). Submarine speed u is relative to the ambient undisturbed fluid. It is also used as a reference speed in various formulations. D_B is linear reference dimension taken here as the diameter of the submarine body.

The ratio of inertial to gravitational forces yields some form of Froude or Richardson number. Gravitational forces arise from variations in fluid density. The following is a densimetric Froude number.

Densimetric Froude number

$$Fr = \frac{u}{\left[g D_B \left(\frac{D_B}{\rho} \frac{\partial \rho}{\partial z}\right)\right]^{\frac{1}{2}}} \tag{2}$$

where $\partial\rho/\partial z$ is fluid density gradient in the vertical direction with positive z downward. g is acceleration due to gravity. Richardson number is the reciprocal square of Fr.

Various features of wake growth and collapse and of internal gravity waves are related to the Brunt-Vaisala time period P given as follows:

$$P = \frac{2\pi}{\left(\frac{g}{\rho}\frac{\partial \rho}{\partial z}\right)^{\frac{1}{2}}} \tag{3}$$

A wave length λ for submarine speed u is given by the following expression.

$$\lambda = uP$$

$$= \frac{2\pi u}{\left(\frac{g}{\rho}\frac{\partial \rho}{\partial z}\right)^{\frac{1}{2}}} \tag{4}$$

A non-dimensional wavelength can be formed by dividing λ with a suitable reference dimension which, for later use, will be taken as the initial wake diameter D_i.

$$\frac{\lambda}{D_i} = \frac{uP}{D_i}$$

$$= \frac{2\pi u}{D_i\left(\frac{g}{\rho}\frac{\partial \rho}{\partial z}\right)^{\frac{1}{2}}} \tag{5}$$

Equation 5 is also a form of densimetric Froude number Fi based on D_i. It is related to Fr as follows:

Densimetric Froude number

$$Fi = \frac{uP}{D_i} \tag{6}$$

$$= 2\pi \frac{D_B}{D_i} Fr \tag{7}$$

Where stratification is obtained by temperature gradient in a wind tunnel, the following relations serve to relate $(1/\rho)(\partial\rho/\partial z)$ to temperature.

$$\frac{1}{\rho}\frac{\partial \rho}{\partial z} = -\frac{1}{\theta}\frac{\partial \theta}{\partial z} \tag{7a}$$

were θ is potential temperature. θ is usually replaced with absolute temperature T. The following equation relates the gradients.

$$\frac{\partial \theta}{\partial z} = \frac{\partial \Gamma}{\partial z} + \Gamma \tag{7b}$$

Γ is the adiabatic gradient which has a value of -.00541 °F/ft. This is negligible compared with $\partial T/\partial z$ values obtained in wind tunnel experiments and may be neglected. Note that herein z is taken positive downward, contrary to meteorological usage.

Another modeling criterion expresses the ratio of two forms of inertia forces caused by differing fluid density. It will first be given by the following momentum flux ratio.

$$\frac{\rho(z)\, u(z)^2}{\rho\, u^2} \tag{8}$$

u(z) is velocity at a given location which is affected by propeller blade forces. $\rho(z)$ is fluid density at the same location. ρ is reference density at the elevation of propeller and body axis (z=0). It will later be shown that for the momentumless condition, the velocity ratio u(z)/u is the same in model and prototype at geometrically similar locations. Thus there remains the density ratio $\rho(z)/\rho$ as a density criterion to be applied at geometrically similar locations. Also shown later is the alternate form of density criterion given in terms of density gradient.

$$\text{Density gradient factor} = \frac{D_B}{\rho}\left(\frac{\partial \rho}{\partial z}\right) \tag{9}$$

Comparison of Equations 2 and 9 shows that another form of Froude number may be used as a velocity criterion as follows.

Velocity Froude number

$$Fr' = \frac{u}{(g\, D_B)^{\frac{1}{2}}} \tag{10}$$

Any two of Equations 2, 9, and 10 will simultaneously satisfy the criteria for gravitational forces and those due to momentum flux.

Results of theoretical and experimental investigations summarized later show that various characteristics of wake collapse beyond a certain distance are dependent primarily on densimetric Froude number Fi (Equation 6). These characteristics are, however, related to an initial wake diameter D_i and virtual origin of streamwise location x (see Figure 1). There is a gap in the knowledge on the relation of D_i and virtual origin location to submarine size and configuration as well as velocity and other operating variables significant to initial wake characteristics. Here the effects of Reynolds number (Equation 1) and the density gradient factor (Equation 9) may be important. Froude number appears to be of lesser importance if not negligible. The relative importance of various criteria changes with distance in this complex transition region. It is important to determine how and to what degree the experimental characteristics for submarines in unstratified flow may be applied to the determination of wake characteristics in stratified flow.

B. Problems of Reynolds Number Modeling

The difficulty, if not impossibility, of satisfying Reynolds number simultaneously with the gravitational and density gradient criteria becomes evident when comparing the requirements of Equations 1, 2, 9, and 10. Fortunately, this does not appear to be necessary. If the density gradient criterion is neglected, Equations 9 and 10 are omitted. There is at least a theoretical possibility of meeting the remaining criteria. The required density gradient, $(1/\rho)(\partial\rho/\partial z)$ for a scale model experiment would, however, reach absurd values.

If Reynolds number (Equation 1) is taken as the only criterion for purposes of studying the immediate downstream wake region, modeling problems are still difficult. To maintain prototype Reynolds number in scale model experiments, the test speed u must be increased to compensate for the

smaller model dimensions. In addition, the difference in kinematic viscosity of air and water must also be taken into account. The following example shows the magnitude of test speeds needed for air at atmospheric conditions. It is assumed that a compressed air type tunnel is not under consideration. For equal Reynolds number, the following relations can be formed. The subscripts "m" and "p" refer to model and prototype, respectively.

$$\frac{u_m}{u_p} = \frac{L_p}{L_m} \cdot \frac{\nu_{air}}{\nu_{water}} \tag{11}$$

At 70°F and 29.92 in. Hg pressure, the ratio of kinematic viscosities $\nu_{air}/\nu_{water} = 15.52$. Assuming a 6ft. long model is used to represent a 300ft. long submarine, the length ratio, $L_p/L_m = 50$. The required velocity ratio u_m/u_p is 776, an impossibly high value. It does not appear feasible to reproduce prototype Reynolds number in model experiments, even when other criteria are neglected.

It is well known in the aerodynamics of various shapes that it is not always necessary to reproduce prototype Reynolds number to obtain useful model data for aerodynamic characteristics. Of fundamental importance is the extent of laminar and turbulent boundary layers over the body surfaces. This affects surface friction drag and, indirectly, the wake characteristics. These depend on Reynolds number but also on body configuration and surface roughness. Propeller forces and induced velocity are largely independent of Reynolds number. Where there is significant dependence of body drag (as expressed by a drag coefficient) on Reynolds number, there are remedial measures. Model configuration including surface roughness can be modified to obtain high Reynolds number characteristics at low model Reynolds number. Other methods of boundary layer control are available. When independence of Reynolds number is achieved, various velocity components in the wake region

tend to be proportional to free stream velocity. This is a characteristic of turbulent wakes.

C. Characteristics and Modeling Criteria for the Close and Near Wake Regions

The close and near wakes are defined as those portions of the wake originating at the body and extending downstream to the region where the effects of gravitational forces first become significant. The distance covered by the close and near wake is variable with densimetric Froude number Fi (Equation 6). The motions are caused primarily by inertial forces arising from body drag and propeller blade forces. As will be shown later, these forces depend on local fluid density as well as velocity. A criterion is developed to account for fluid density variation.

The motions induced by inertial type forces occur immediately with their occurrence. They account for close and near wake characteristics. Motions due to gravitational forces require time for development of their effects. While such forces exist in the close and near wake, their effects become felt later.

The initial wake characteristics are developed in the close and near wake regions where the configurations of the body and propeller have the greatest influence. The near wake is a transitional region where the details of propeller and body induced motions become merged into a more general momentumless wake flow. The following elementary analytical treatment serves to bring out some major features of propeller induced speeds and provide the basis for the development of the density criterion. Figure 1 shows the set up of the various components of the flow field around and through the propeller. The speed induced by propeller thrust will be obtained by the simple momentum theory. The thrust T is assumed to be produced by an "actuator disk" at which the pressure increment Δp occurs. This will first be developed for unstratified

flow (ρ = constant). The effect of body drag on the stream approaching the propeller is represented by speed u_a which is less than free stream speed u. For turbulent boundary layer and wake, u_a tends to be proportional to u. The effect of the pressure field caused by flow distortion of the body tends to produce speed changes proportional to u and is viewed as incorporated in u_a. Cross section "a" and "w" are sufficiently far upstream and downstream, respectively, to be unaffected by the pressure field of the propeller. Their cross sectional areas are those of the stream tube of fluid passing through the propeller disk.

Propeller thrust T is found with the following equation which is the difference in downstream and upstream momentum flux. Figure 2 shows various characteristics.

$$T = \rho A_w u_w^2 - \rho A_a u_a^2 \tag{12}$$

The following relationships are obtained from the equation of continuity.

$$\begin{aligned} A_a u_a &= A_p u_p = A_w u_w \\ &= A_p(u_a + \Delta u_p) = A_w(u_a + \Delta u_w) \end{aligned} \tag{13}$$

Thrust T can be written in terms of disk area A_p as follows:

$$T = \rho A_p(u_a + \Delta u_p)\Delta u_w \tag{14}$$

The following relationship can be found by application of Bernoulli's equation to the upstream and downstream regions.

$$\Delta u_p = \frac{\Delta u_w}{2} \tag{15}$$

Thus T can be expressed in terms of the induced speed Δu_w in the propeller slipstream.

$$T = \rho A_p\left(u_a + \frac{\Delta u_w}{2}\right)\Delta u_w \tag{16}$$

The non-dimensional thrust coefficient C_t is defined in terms of the free stream

speed u as follows:

$$T = C_t \frac{\rho u^2}{2} A_p \tag{17}$$

C_t is related to Δu_w as follows:

$$C_t = 2\left(\frac{u_a}{u}\right)^2 \left(1 + \frac{\Delta u_w}{2u_a}\right) \frac{\Delta u_w}{u_a} \tag{18}$$

The speed ratio $\Delta u_w/u$ induced by the propeller is as follows:

$$\frac{\Delta u_w}{u} = -\frac{u_a}{u} + \sqrt{\left(\frac{u_a}{u}\right)^2 + C_t} \tag{19}$$

The momentumless condition will be introduced with a drag coefficient C_D for body drag D defined as follows:

$$D = C_D \frac{\rho u^2}{2} A_B \tag{20}$$

where A_B is body frontal area $\left[= (\pi/4) D_B^2\right]$. The momentumless condition is given by equality of thrust and drag.

$$T = D \tag{21}$$

Thrust coefficient C_t is related to drag coefficient C_D as follows:

$$C_t = C_D \frac{A_B}{A_P} \tag{22}$$

When substituted into Equation 19 the following is found for induced speed ratio.

$$\frac{\Delta u_w}{u} = -\frac{u_a}{u} + \sqrt{\left(\frac{u_a}{u}\right)^2 + C_D \frac{D_B^2}{D_P^2}} \tag{23}$$

For turbulent flow, C_D and u_a/u tend to be constant. Thus the speed induced by the propeller is proportional to free stream speed as is the speed defect due to body drag.

The effect of fluid density variation will be found by consideration of

the flow through a stream tube which encloses the element of area dA_p at the propeller (see Figure 2). Thrust dT on this element produces induced wake speed $\Delta u_w(z)$ which may be dependent on elevation. The local thrust coefficient C_{te} is defined by the following equation which is similar to Equation 17 for the entire propeller.

$$dT = C_{te} \frac{\rho u^2}{2} dA_p \tag{24}$$

ρ is now reference density on the longitudinal axis (z=0). The following equation for local thrust coefficient is similar to Equation 18.

$$C_{te} = \frac{2\rho(z)}{\rho} \frac{u_a^2}{u^2} \left(1 + \frac{\Delta u_w(z)}{2 u_a}\right) \frac{\Delta u_w(z)}{u_a} \tag{25}$$

The induced speed ratio in the element wake is given by the following equation

$$\frac{\Delta u_w(z)}{u} = -\frac{u_a}{u} + \sqrt{\left(\frac{u_a}{u}\right)^2 + C_{te} \frac{\rho}{\rho(z)}} \tag{26}$$

This equation is similar to Equation 19 for unstratified flow except for the density ratio $\rho/\rho(z)$. It is not appropriate to introduce drag coefficient C_D as was done for the entire propeller since C_{te} may vary over the propeller disk. It will, however, be proportional to drag coefficient. For similarity of the induced speed field, $\Delta u_w(z)/u$ must be the same in the model and prototype at geometrically similar locations. This will be obtained if $\rho(z)/\rho$ is the same at geometrically similar locations. This requirement can be expressed in terms of fluid density gradient $\partial\rho/\partial z$ as follows. For simplicity the gradient is assumed to be constant by the following equation.

$$\rho(z) = \rho \frac{\partial \rho}{\partial z} z \tag{27}$$

The following form gives the density ratio as it appears in the inverse ratio in Equation 26.

$$\frac{\rho(z)}{\rho} = 1 + \frac{1}{\rho} \frac{\partial \rho}{\partial z} z \tag{28}$$

In order to emphasize the density ratio at geometrically similar locations, Equation 28 is written with elevation z non-dimensionalized with body diameter.

$$\frac{\rho\,(z/D_B)}{\rho} = 1 + \frac{D_B}{\rho}\frac{\partial \rho}{\partial z}\left(\frac{z}{D_B}\right) \tag{29}$$

The density criterion is the factor in the second term on the right side of Equation 29 which produces density similarity.

$$\text{Density gradient factor} = \frac{D_B}{\rho}\left(\frac{\partial \rho}{\partial z}\right). \tag{30}$$

The importance of the density gradient criterion remains to be established. This will, obviously, require scale model experiments with propulsive forces in stratified flow. Momentum effects due to propulsive forces are likely to occur in a relatively short downstream distance in the close and perhaps the near wake. In these regions the initial wake diameter D_i is determined. It depends on propulsive forces and submarine configurational features. In the intermediate and far wake regions, propulsive forces may have an indirect effect through the magnitude of D_i which appears in the equations for these regions.

D. Intermediate and Far Wakes

The major effects of gravitational forces occur in the intermediate and far wake regions. Wake coliapse occurs in the intermediate wake followed with continued horizontal wake growth in the far region. These are shown schematically in Figure 3.

Geometric properties of the intermediate and far wakes will be discussed in terms of the summary curves of G. F. Merritt (Reference 1). An extensive list of references is included. He bases these curves on various experimental and theoretical inve-tigations. They show the importance of densimetric Froude number (Equation 6) in the modeling of intermediate and far wake regions. Figure 4 shows the wake width and height as a function of time after

wake generation. It is a reproduction of Figure 14 of Merritt's paper. Merritt's equations representing various portions of the curves are given below. The wake widths and heights are non-dimensionalized with the initial wake diameter D_i. The time variable t is non-dimensionalized with the Brunt-Vaisala period P (Equation 3). Approximate values of t/P ranges for each width or height equation are taken from Figure 4.

Horizontal and vertical width:

$$b_\infty/D_i = 1.3\ Fi^{1/4}\ (t/P)^{1/4}$$

$$t/P \leq 0.2 \qquad (31)$$

Horizontal width:

$$b_h/D_i = 2.0\ Fi^{1/4}(t/P)^{-3/4}$$

$$0.2 \leq t/P \leq 1.0 \qquad (32)$$

$$b_c/D_i = 2.0\ Fi^{1/4}(t/P)^{1/4}$$

$$1.0 \leq t/P \qquad (33)$$

Vertical width:

$$b_m/D_i = 0.9\ Fi^{1/4}$$

$$0.2 \leq t/P \leq 0.45 \qquad (34)$$

$$b_v/D_i = 0.5\ Fi^{1/4}(t/P)^{-3/4}$$

$$0.45 \leq t/P \leq 1.0 \qquad (35)$$

$$b_f/D_i = 0.5\ Fi^{1/4}$$

$$1.0 \leq t/P \qquad (36)$$

In terms of the preceding wake descriptions, Equation 31 is in the near wake, Equations 32, 34, and 35 are in the intermediate wake and Equations 33 and 36 in the far wake.

The three-dimensional geometry is emphasized by rewriting the above

equations in terms of downwind distance x which is related to time t and speed u as follows:

$$t = x/u \tag{37}$$

$$t/P = x/uP$$

$$= (x/D_i) \cdot (D_i/uP) \tag{38}$$

$$= Fi^{-1}(x/D_i) \tag{39}$$

Equations 31 through 36 are as follows in terms of distance ratio x/D_i.

$$b_\infty/D_i = 1.3\ (x/D_i)^{1/4} \tag{40}$$

$$b_h/D_i = 2.0\ Fi^{-1/4}(x/D_i)^{1/2} \tag{41}$$

$$b_c/D_i = 2.0\ (x/D_i)^{1/4} \tag{42}$$

$$b_m/D_i = 0.9\ Fi^{1/4} \tag{43}$$

$$b_v/D_i = 0.5\ Fi\ (x/D_i)^{-3/4} \tag{44}$$

$$b_f/D_i = 0.5\ Fi^{1/4} \tag{45}$$

Merritt's analysis of various data shows no consistent dependence of wake diameter on Fi in the near wake. This is reflected in above Equation 40 which does not have a Fi dependent factor. Location of downstream range of the near wake is, however, dependent on Fi since this is given at $t/P = 0.2$. It is given by the following equation

$$x/D_i = Fi(t/P)$$

$$= 0.2\ Fi \tag{46}$$

With decreasing values of density gradient $\partial\rho/\partial z$, Fi and, therefore, x/D_i increases indefinitely.

The above equations for wake geometry show a dependence on Fi in various forms. For geometric simularity, Fi becomes the only modeling

criterion. The above data give no information which would relate the initial wake diameter D_i to actual body diameter D_B. Also unspecified is the location of the origin of the coordinates, a virtual origin. These are dependent on close and near wake characteristics.

III. Description of the Environmental Wind Tunnel

The main features of the Environmental Wind Tunnel other than those covered in later sections are described in the following paragraphs. Those described later are modifications or developments made specifically for this project.

The Environmental Wind Tunnel is located in the Preston R. Bassett Aerospace Research Laboratory at the Long Island Center in Farmingdale, New York. The wind tunnel (Figure 5) is of the open circuit type in which air is drawn from the laboratory room into the contraction cone and exhausted back to the room. Following the contraction cone or bell mouth (constructed of wood) the air enters the rectangular test section which is 5 ft. wide and 4 ft. high. A vertical bank of electric heaters is located 3 ft. into the test section. It is described in Section IV, A. It is the only apparatus permanently fixed in the test section. The mean wind profile generator shown in Figure 5 was not installed for this project since a constant velocity profile was desired.

Test section length downstream of the heater section is approximately 21 ft. The floor and ceiling and the first 8 ft. of the walls including the part upstream but excluding the heater section are made of 3/4 in. plywood. The heater section is made of 3/8 in. aluminum plate. The remainder of the walls is formed of Pittsburgh Plate Glass thermopane glass panels (double glass). The walls, ceiling, and the remaining downstream section are supported with structural steel framework. The 9.5 ft. long plywood transition section between the test section and fan contains the access door. The photograph of Figure 6 shows

various instruments located alongside the test section. Other views of the test section are shown in Figures 26-29.

The American Standard model 940 centrifugal fan draws the air through the various upstream sections. The General Electric Varidrive system powers the fan with a multiple V belt drive. The system consists of a variable speed D. C. motor and a solid state controller which converts the A. C. input to variable D. C. Air speed is continuously variable from 0.25 ft/sec to approximately 30 ft/sec, the maximum obtainable with only the heater section in place. Speed regulation is excellent. Additional wind tunnel details are given in Reference 2.

Vertical profiles of air speed on the test section vertical centerline are shown in Figure 7. They were taken 9.9 ft. downstream of the heater section without heat input from the airstream heaters. Air speed was measured with Pitot-static tubes and the MKS Baratron pressure meter (see Section IV, D). Except for the 1 inch level measurement in the floor boundary layer, the values are generally within 3% of the average. This could be improved, but in view of the more difficult problems with effect of stratified flow on air speed distribution, no effort was devoted in this direction. The seemingly inconsistent variations in air speed profiles may have been caused by time variation in laboratory room thermal conditions.

IV. Equipment Development and Experimental Characteristics

A. Airstream Heaters and Temperature Profiles

An important feature of the wind tunnel needed to meet the air density gradient requirement for stratified flow is the control of airstream temperature gradient. A vertical bank of General Electric Calrod electric heaters is located at the upstream end of the test section as shown in Figure 5. The heaters are of the finned rod type which span the 5 ft. width of the airstream. Electric current is supplied to the terminals at the ends of the heaters located

outside of the test section walls. Four solid state West Instrument power controllers with thermocouple airstream sensors automatically control heater output to the four overlapping groups of heaters.

The heater system must supply controlled heat input such as to produce a desired linear profile for lengthy time periods as needed for the many air speed and temperature measurements of a test run. This period may be as long as 2 or 3 hours. During this time, thermal conditions in the laboratory may change due to variations in space heating and changes in wall and ceiling temperatures caused by outside atmospheric conditions. Since the wind tunnel is of the open circuit type, temperature variations in the laboratory room air are carried into the wind tunnel test section. The heaters must compensate for these temperature variations in addition to producing the desired temperature profile.

The principle for heater circuit design is shown schematically in Figure 8 where calculated heat profiles are shown. Each of four overlapping groups of heaters produce triangle shaped heat input profiles. Temperature profiles will be similar since the distribution of the mass flow of air is approximately uniform except near the floor and ceiling. Each group has its own thermocouple sensor located at the peak of the triangle. The adjacent groups have the edges of their heat triangles near the thermocouple and will, therefore, have little effect on them. Thus the thermocouple controls the group it is connected to and has little interference from adjacent groups. The thermocouples are located 13 inches downstream of the heaters. With this arrangement of overlapping groups, a linear profile of heat input can be obtained. A calculated linear profile is shown in Figure 9. In operation, the power controllers are set to produce temperatures at the thermocouples which are on a linear profile. Non-linear profiles can also be produced but in linear segments between thermocouples. Discontinuities in the gradient of the heat

input profile are smoothened out in the downstream temperature profiles due to heat diffusion.

There are 54 heaters in the heater section. Forty-seven are in two vertical staggered banks at 2 inch spacing in each bank to give 1 inch vertical spacing of the combined banks. They cover the full height (48 in.) of the test section. There is an additional bank of 7 heaters at 2 in. spacing down from the ceiling to give additional capacity where most needed for a stable temperature profile.

In order to obtain a triangular heat input profile, the individual heaters must operate at differing voltages. To avoid having a large number of external circuit elements such as resistors or transformers, the various heaters in a group were connected in various combinations of series and parallel sub-circuits. These are shown in Figures 10a and 10b. These were devised by a trial and error process. Heaters numbered 1 through 47 are in the two vertically staggered banks with no. 1 at the bottom. Heaters numbered 48 through 54 are in the additional upper bank with no. 48 at the top. For simplicity of analysis, the calculation of electric input was based on heater resistance of 1 ohm and input voltage of 1 volt. The graphs of Figures 8 and 9 show values termed "unit watts" which are later scaled up for actual input values. In operation, the power controllers supply electric power at any value up to their capacity as determined by the thermocouple sensors.

Measured temperature profiles for individual and combined heater groups in operation are shown in Figure 11. These were made to demonstrate heater operation early in the experimental program before better operating techniques were developed. Figure 12 shows profiles at three cross stream locations which show little cross stream variations. These were obtained at an air speed of 2.5 ft/sec. At speeds below 1.5 ft/sec uniformity of flow deteriorates. This is due to vertical variation of pressure drop across the heater section. To improve this condition, a flow equalizer plate was installed upstream of the heater section. This is described in Section IV, C.

B. Smoke Generator

The introduction of smoke streamers in the test section aids in the study of flow characteristics. While the test speeds used in these experiments are low, they are not low enough to obtain pure laminar flow and smooth smoke filaments which are characteristics of specially designed smoke tunnels. Smoke streamers produced in the Environmental Wind Tunnel tend to break up into puffs especially with dense smoke for which gravitational forces are significant. The streamers do, however, maintain sufficient identity to show flow patterns. Observation of the relative motion of puffs gives an indication of relative speeds of various sections of the airstream. For air speeds below 5 ft/sec. the motion of smoke puffs was used to calibrate the air speed instruments. Time of passage of a puff was observed over a measured distance within the 16 ft. length of the glazed test section wall.

Smoke was injected into the wake of the disk model described in Section V.

The smoke generator built for this project is shown in Figures 13 and 14. Fog oil (Mole-Richardson Type 1964 Fog Juice) is fed into the vaporizer section from an elevated tank. An electric heating coil vaporizes the oil. As the vapor issues from the orifice it condenses in the air passing through the generator to form a dense white smoke composed of small oil droplets. Air comes from a compressed air supply. Smoke is produced continuously as long as needed.

C. Low Speed Characteristics and Development of Flow Equalizer Plates

Up to this point in project activities, various temperature and air speed measurements with heaters on were made at air speeds of 2.5 ft/sec. and higher. Various equipment problems had been solved for these speeds. It was evident that uniformity of air flow in the test section deteriorated as air speed was lowered. Measurements of air speed and temperature became irregular. Air speed measurements with a Pitot-static tube were difficult to obtain due to wide fluctuations in readings (see Section IV, D). Following

preliminary wake experiments, the size of disk needed for final experiments was tentatively determined. For this size the air speeds must be below 2 ft/sec., preferably 1 ft/sec., for significant features of wake collapse to occur within the length of the available test section. The final wake experiments (Section V) were conducted at 1.25 ft/sec.

Owing to the difficulties in obtaining low air speed measurements, it was descided to construct the smoke generator described in Section IV, B so that visualization of air flow could be obtained. With smoke streamers it was found that below 1.5 ft/sec. (with heat input) air speed variation was highly irregular. There was a stagnant region near the central region of the test section starting several feet downstream of the heaters. There was a slow downstream movement below the stagnant region and higher speed downstream movement above the stagnant region. Additional smoke streamers close to the heaters showed a marked upward component of motion in the upper region. Further exploration with smoke streamers at the heater section showed a reversal of flow in the upper several inches adjacent to the ceiling. Smoke flowed upstream through the heaters and followed the ceiling of the contraction cone out into the room.

It was expected that there would be vertical variation in pressure drop across the heater section due to the vertically variable temperature difference across the heaters, but the magnitude of this effect on airspeed profile was not realized. Elementary calculations on this effect showed qualitative agreement with smoke flow observations. Pressure taps were installed on one wall of the test section upstream and downstream of the heaters. Results of pressure drop measurements with and without heat are given in Figure 15. Differences between heat on and heat off values are shown on the left side. of the figure. Similar pressure difference profiles were obtained for speeds of 1.0, 1.5, and 2.0 ft/sec. The markedly different result for 3.0 ft/sec.

was rechecked but not explained. Since the speeds of interest were lower, the reason for this deviation was not pursued.

It was evident that some form of additional pressure drop was needed to eliminate pressure reversal. A vertically variable pressure drop to match that produced by heaters would be ideal,but this required complex equipment beyond the scope of this project. It was decided to use a uniform pressure drop which at 1.5 ft/sec. would produce values comparable with those of the heaters at 3.0 ft/sec. shown on Figure 15. The needed pressure drop was higher than that obtained from commercially available screens. The needed value was obtained with a perforated plate. It was made of aluminum sheet drilled with 0.5 in. dia. holes in a uniform pattern which gave a solidity (sheet area remaining) of 70%. This gave a pressure drop coefficient of 15. The plate was located shortly upstream of the heater section.

Pressure drop data obtained with and without the equalizer plates are shown in Figure 16 for a speed of 1.5 ft/sec. Visual observation of smoke streamers showed that, with heat on, air speed was higher in the upper part of the test section. Measurements with a Pitot-static tube were of limited accuracy but confirmed the trend observed with the smoke streamers. The propeller anemometer used in the later experiments had not been developed at this stage. A vertically non-uniform pressure drop was needed. To this end, horizontal lines of the equalizer plate holes were blocked out in the upper portion. This trial and error process produced a uniform air speed profile for a given speed setting. For another speed, the blockage pattern was different. Testing at a series of speeds was, therefore, quite time consuming. There is the need for a flow equalizer plate with vertically variable solidity which can readily be adjusted.

D. Air Speed Measurements with Pitot-static Tubes and Contraction Cone Orifices

Prior to this project, air speeds in the test section were generally measured with Pitot-static tubes. The test speeds were well above those needed for this project. Speeds below 3 ft/sec. needed for this project are often considered too low for Pitot-static tubes due to the very low pressure difference obtained and possible Reynolds number effects which could change the calibration. There was available a MKS Baratron Type 77 pressure meter which, on the most sensitive range, could indicate the pressure difference produced by the Pitot-static tube. At 1.5 ft/sec. this difference (dynamic pressure) is 0.002,57 lbs/sq.ft. and 0.001,14 lbs/sp.ft. at 1 ft/sec. Pitot-static tube calibration was checked by measurement of test section air speed with time of travel of smoke puffs over a measured distance.

To obtain true air speed from Pitot-static tube readings and from contraction cone pressures described below, it is necessary to have the air density. This could be obtained from readings of barometric pressure, temperature, and humidity. The wind tunnel elevation is close to sea level. The assumption of standard sea level air density as used in all calculations does not lead to errors beyond the accuracty of other measurements.

There is some spatial variation in test section air speed (Figure 7). To avoid the averaging of a number of reading as was done for Figure 7, it was decided to base the reference speed on the pressure difference obtained between the beginning and end of the contraction cone. This is a common procedure in subsonic wind tunnels. The pressure difference is a little less than that obtained with a Pitot-static tube but it appeared adequate with the use of the Baratron pressure instrument. Orifices were installed in the contraction cone.

The Pitot-static tube used in the first calibration experiments had a

diameter of 1/8 in., a standard size for the various aerodynamic laboratories at Polytechnic. At air speeds of 1.5 ft/sec. and lower, the Baratron indicator showed large amplitude fluctuations with periods of a second or more which increased with decreasing speed. On a strip chart recorder at 1 ft/sec. air speed the amplitudes were as high as 5 times the mean value of the reading, extending well into the negative range. Observation of smoke streamers showed no evidence of speed fluctuations at the Pitot-static tube. An additional problem was the zero drift of the instrument.

It seemed that the cause for the fluctuations was occurring between the Pitot-static tube and the pressure measuring unit of the Baratron. The small orifices of the 1/8 in. Pitot-static tube would restrict any flow out of the tubing which might be caused by change in air volume due to temperature variations. A 1/4 in. dia. Pitot-static tube was tried, then one of 1/2 in. dia. These had larger orifices. The 1/8 in. dia. plastic tubing was replaced with 1/4 in. dia. The plastic tubing was then replaced with 1/4 in. copper tubing. Each of the changes resulted in some reduction in amplitude of fluctuations, but it was far from satisfactory. Pressure readings of the orifices in the contraction cone showed similar fluctuations, but a little lower in magnitude.

On the basis that the fluctuations were due to changes of air volume in the lines, it was decided to insert constant temperature air chambers in the lines. Constructed of brass, each chamber had a volume of 71 cu.in. (1.16 liters) which is many times the air volume in the lines. They were place in a water bath at room temperature. The chambers reduced the fluctuations to 1/4 or less of the original magnitude. This was acceptable. The water bath container is seen at the lower left of the photograph in Figure 6.

With the reduction in short period fluctuation there emerged quite regular longer period (several minutes) fluctuations. These were sufficiently large that the strip chart record had to be averaged over a period of time.

These fluctuations seem to be a characteristic of the instrument when used on its most sensitive range.

These longer period fluctuations together with zero drift required a chart record of 15 to 20 minutes to obtain a good average reading. This was satisfactory for measuring and monitoring the contraction cone pressure difference while obtaining point by point measurements in the test section. Preliminary wakes experiments showed it was too time consuming for point by point air speed measurements with a Pitot-static tube. For this reason, the propeller anemometer described in Section IV, F was developed.

E. Survey Carriage

The preliminary temperature profile measurements were made with the available vertical array of thermocouples mounted on streamline tubing at fixed locations. This proved unsatisfactory for the later more extensive profile measurements of air speed and temperature. Remote control and flexibility of probe position was needed to reduce experimental time and to avoid disturbing the airstream each time a probe position was changed. The first version of the survey carriage provided remotely controlled vertical position of a thermocouple and Pitot-static tube simultaneously. The carriage base rested on the test section floor and padded screws pressed against the ceiling. The first version consisted of those parts excluding the horizontal traversing section shown in the photograph of Figure 17.

With the preparations for the disk wake experiments, the horizontal section was added to provide remote control of horizontal and vertical positions. Two variable speed D. C. motors drive the horizontal and vertical lead screws. A solid state controller provides the variable D. C. input for the motors.

F. Propeller Anemometer

Propeller (or vane) anemometers used in meteorological field experiments have low threshold air speeds. Their size is much too large for wake

measurements where the ideal is the air speed at a point. While low speed instruments with small probes are commercially available, they are costly and have electronic circuitry which can have operational problems of the type encountered with the Baratron pressure instrument. Propeller type anemometers are used in heating and ventilating studies but they are also quite large. It was decided to try the construction of a small version of the meterological propeller anemometer. It would be a simpler instrument with little maintenance. As the diameter is reduced, threshold speed tends to increase due to change in relative magnitude of aerodynamic torque and bearing friction. While there was no guide on the allowable diameter to obtain good wake speed measurements, it was thought that a 1 in. diameter would be adequate. It was designed to obtain wake readings at distance intervals not larger than 2 in. Various materials for blade construction and types of bearings were tried. The final version is shown in the photograph of Figure 18. It has 6 blades and a diameter of 1.63 in. The blades were individually carved from solid balsa wood to a thickness of approximately 1/32 in. The blades were glued to a shaft which is supported in 0.014 in. dia. jewel bearings.

Since the aerodynamic torque is very low, it could not be used to drive any kind of generator. For these experiments, rotational speed of the propeller was obtained with visual observations. The number of revolutions were counted for a 30 sec. period. The calibration curves are shown in Figure 19. The final version shows a threshold air speed of 0.6 ft/sec. This is a little lower than the lowest wake speeds shown in Figures 17, 18, and 19. These data do not suggest that the 1.63 in. dia. anemometer is to large for these experiments. The intermediate calibration was obtained before certain refinements were made. The light lubricating oil used in the intermediate version was replaced with clock oil. Static balance of the anemometer was improved. Surface smoothness of the blades was also improved. The

calibration data taken before and after the final series of experiments (Figures 17, 18, and 19) showed little, if any, change in calibration. Included is a curve for the anemometer axis yawed 20°. This was obtained for the conditions of the intermediate calibration.

Visual counting of anemometer revolutions was feasible within the speed range shown in Figure 19. The rotational speed was too low for use of a stroboscope. An improvement in measuring rotational speed would be the use of a tachometer which indicates the interruptions of a light beam projected through the plane of the blades. This would reduce the time for obtaining a reading. Further experimentation with blade shape, number of blades, and bearings would probably yield improved performance.

V. Disk Wake Experiments

The experiments on wake collapse were made with a perforated disk of 8 in. dia. While the ultimate objective is the study of momentumless wakes, this would at this stage introduce the complications of thrust production. Some important characteristics of wake collapse in stratified flow can be studied with a disk model as is shown with the data presented herein. Wake mixing makes wake stratification less than in the surrounding region. This produces cross-stream horizontal buoyancy forces which cause horizontal spreading. To further increase wake mixing, rotation vanes were installed behind the disk. The disk is perforated with a number of holes to reduce drag and turbulent oscillations in the wake. Disk and vanes are shown in Figure 20.

Wake dimensions are based on horizontal and vertical air speed profiles taken on lines through model centerline. Profiles were measured with the propeller anemometer at distances of 4 ft. and 8 ft. downstream of the disk. Problems with holding temperature profiles made it difficult to obtain the same profile over extended time periods needed for air speed and temperature measurements. The problem was aggravated by the high indoor and outdoor

temperatures. Two temperature profiles are shown in Figure 21. They were obtained on different days. The breaks in the curves are due to discontinuities in the order of taking measurements and time interval between reading the upper and lower portion of the curve. The lower portions of the curves tend to a value 90°F which was close to the laboratory room temperature. Under more favorable conditions, profiles of the form shown in Figure 12 would be obtained. The linear portions of the curves have temperature gradients close to 10°F/ft. which was taken as the gradient representative of these experiments. The free stream air speed was 1.25 ft/sec. Model temperature of 98° was used in calculating the parameters in the following paragraph.

Densimetric Froude number Fr given by Equation 2 has a value of 2.47 for these experiments. Densimetric Froude number Fi as used in Merritt's paper (Reference 1) given by Equation 7 has a value of 15.5. Wake diameter D_i and body diameter D_B are assumed equal. For the disk model the wake starts at the outer edge of the disk. Fr and Fi differ by a factor of 2π. The Brunt-Vaisala time period P (Equation 3) has a value of 8.28 sec.

In spite of the finite diameter (1-5/8 in.) of the propeller anemometer, good air speed profile measurements were obtained. These are shown in Figures 21, 22, and 23. For the purpose of direct comparison of various profiles in Figure 25, some of the measured profiles were adjusted by multiplying the air speed defect in the wake by a constant as needed to make minimum wake speed the same. The center of the wake as shown by the lowest air speed location was displaced from the model centerline about 3 in. at the 8 ft. distance, an angle less than 2°. The wake profiles are plotted to a common centerline in Figure 25.

For purpose of comparison with data from other sources, Figure 14 of Merritt's paper (Reference 1) is used. This is the same as Figure 4 of this report. It is a composite of results given in various papers. Nearly all are

based on experiments conducted in water. Merritt's non-dimensional Figure 14 is reworked into a dimensional form for the conditions of these experiments and plotted in Figure 24. Numerical values were obtained from Equations 40 - 50 of this report which represent Merritt's figure. Figure 24 shows actual downwind distance and wake half widths. The neutral case is taken from Merritt's Figure 2 (Reference 1). Merritt's wake widths from Figure 24 are plotted in Figure 25 for the 4 and 8 ft. downstream distances.

It is difficult to define the wake widths obtained in these experiments because of the asymptotic nature of the air speed profile, thus no experimental half widths are shown. This depends on interpretation of the profiles. The symbols show Merritt's values but they also serve to identify the experimental profiles. In the case of horizontal width with stratified flow at x = 4 ft. the wake half width (approx. 20 in.) is much larger than Merritt's values. There is a marked change in slope which occurs at Merritt's half width (approx. 10 in.). For other profiles there is substantial agreement with Merritt's values. Comparison of the vertical profiles-stratified flow at 4 and 8 ft. distances shows no actual indication of wake collapse as predicted by Merritt's curve shown on Figure 24. Wake height is approximately the same. It is, however, much less than that for neutral flow. It is possible that the rotation vanes behind the disk produced too much turbulence. This would oppose the collapsing action. The plain perforated disk was observed with smoke in the wake but air speed profiles were not measured. It seemed that more turbulence was needed, thus the vanes were added. Another disk solidity might be better. Other means of increasing wake turbulence such as oscillating the disk might be better. Merritt used this technique in his experiments. It is evident that more experimentation is needed. Variables such as test speed and temperature gradient should be vaired over a range of values. More downstream distances should be included. Profiles should be taken at other than centerline location to

define wake cross sectional shape. Unfortunately, the experimental phase of the project was terminated at this point. These experiments are really preliminary in character. Numerous experimental problems discussed in other sections of this report had been solved in preparation for the wake experiments.

The photographs of Figures 26 - 29 show the wakes with smoke introduced immediately behind the disk. Smoke is conducted through the pipe which supports the disk model. Unfortunately the smoke is not highly visible. A dense smoke would tend to fall. The time of travel over the 8 ft. distance, approximately that covered in the side view photographs Figure 26 and 27, is over 6 sec. A dense smoke forms inverted mushroom type puffs which fall. The relatively short camera exposure time gives a near instantaneous view of the fluctuating wake compared with the 30 sec. average obtained with air speed data obtained with the propeller anemometer. However, 30 sec. is not needed to obtain a good average. Perhaps several seconds would suffice. A camera time exposure over that time period would give an average but such photographs lack definition of wake edge. A better procedure is the multiple exposure technique where a number of instantaneous exposures are made on the same film. The author used this technique quite successfully in field experiments on smoke plumes at the Argonne National Laboratory. Wind tunnel application of this technique requires special lighting. Such data would be an excellent supplement to the velocity profile data. Another technique is the use of a detectable gas tracer in place of smoke. The gas concentration profiles which could be obtained with suitable instrumentation would help define wake outline.

It is to be noted that Merritt's values are a composite of various experiments from various sources including his own hydrodynamic experiments. A survey of the various data sources might reveal some which show better agreement with the results obtained in this project. The bulk of

Merritt's data was obtained with hydrodynamic experiments. The substantial agreement of the wind tunnel data obtained in this project shows that air is an effective substitute for water in the study of wakes in stratified flow. It has important experimental advantages pointed out in the introduction.

Some of the air speed profiles of the various profile figures show some decrease of velocity with radial distance outside of the wake. Others may also show this feature if the profiles were carried out far enough. The flow near a blunt body usually shows an increase in air speed near its maximum width outside of the boundary layer. This effect may have persisted some distance downstream of the disk model.

Comparison of air speed above and below the wake for vertical profiles shows higher speeds above the wake. It was pointed out in Section IV, C that a constant velocity profile could be obtained with adjustment of the blockage on the orifice plates. Under the time limitations for completion of the wake experiments this refinement could not be made.

VI. Discussion

The final wake experiments on a disk model, summarized in Figure 25, are limited in scope but show the feasibility of using a wind tunnel to study wakes in stratified flow. The substantial agreement of wake widths and heights with Merritt's (Reference 1) largely hydrodynamic data indicates that the use of air in place of water has good potential for investigating various aspects of submarine wakes in stably stratified ocean waters. It is believed that further experimentation and refinement of equipment and techniques will give better results than shown herein. Unfortunately, the lengthy period of experimental preparations left little time for the final wake experiments. Thus they are in the form of preliminary experiments.

The various equipment developed or modified for this project resulted in wind tunnel capability for producing a controlled stably stratified airstream

at speeds as low as 1 ft/sec. There seems to be no serious problems in obtaining lower speeds as may be needed for testing a submarine model with a propulsive unit for producing a momentumless wake. Many of the experimental difficulties were caused by the vertically varying pressure drop across the heater section. The flow equalizer plate was effective in compensating for the varying pressure. Another problem was that of measuring low air speeds. It was solved with the development of the small propeller anemometer. Additional development or refinement of equipment would serve to reduce testing time and to obtain lower air speeds.

The available data from other investigations as given by Reference 1 require only the densimetric Froude number (Equation 2) as the modeling criterion.

$$Fr = \frac{u}{\left[g\, D_B \left(\frac{D_B}{\rho} \frac{\partial \rho}{\partial z} \right)\right]^{\frac{1}{2}}} \tag{2}$$

In terms of model temperature gradient, it has the following form

$$Fr = \frac{u}{\left[g\, D_B \left(- \frac{D_B}{T} \frac{\partial T}{\partial z} \right)\right]^{\frac{1}{2}}} \tag{47}$$

In the final experiments, $\partial T/\partial z = -10^{\circ}F/ft.$ was used because it was readily obtained with the heater section. This, together with the 8 in. dia. disk model and air speed of 1.25 ft/sec., gave Fr values which cover downstream distances where effects of stratification would be well developed. This is shown on Figure 24. The same Fr value could be obtained with lower $\partial T/\partial z$, but the speed must also be lower. It was feared that the speed measurement problem for lower speeds would require more development of speed instrumentation.

The above experimental values may not be in the correct range for

submarine modeling if the additional criterion developed in Section II is important. In that case, Equations 9 and 10 are the criteria as follows:

Velocity Froude number.

$$Fr' = \frac{u}{(g\, D_B)^{\frac{1}{2}}} \tag{10}$$

Density gradient factor.

$$\frac{D_B}{\rho} \frac{\partial \rho}{\partial z} \tag{9}$$

Density gradient factor has the following form in terms of model temperature gradient.

$$-\frac{D_B}{T} \frac{\partial T}{\partial z} \tag{48}$$

To evaluate these criteria for model test values, some prototype values must be used. Typical values for $(L_B/\rho)(\partial\rho/\partial z)$ have been given as 10^{-3} to 10^{-4} where L_B = 100m., the length of submarine body. These result in density normalized gradient $(1/\rho)(\partial\rho/\partial z) \approx 10^{-5}$ to 10^{-6} m^{-1}. Perhaps higher values may be encountered. If a layer of water 30 m. deep has a density which varies from that of fresh water at the top to that of ocean salt water at the bottom, the density normalized gradient is more than an order of magnitude higher than 10^{-5} m^{-1}. Consider the possible model test values for $(L_B/\rho)(\partial\rho/\partial z) = 10^{-3}$. D_B in Equations 10 and 48 may be replaced with L_B for model-prototype comparison. For a model length $L_B \approx 2$ ft., the model temperature gradient must be -0.28°F/ft. to satisfy density gradient factor (48). This compares with the much larger -10°F/ft. used in the disk experiment. If a prototype speed of 50 ft/sec. (29.6 knots) and L_B = 100 m. are used, then the model test speed must be 0.30 ft/sec. to satisfy Equation 10. This compares with 1.25 ft/sec. of the disk experiments. No wind tunnel experiments were conducted in these low ranges. The lower temperature gradient can

be obtained. The principal difficulty appears to be the measurement of the lower air speeds. The importance of the additional criterion requires experimental verification with momentumless wakes in stratified flow. It may be that some departure from required test values is permissible and may depend on such design features as ratio of propeller diameter to body diameter as well as density gradient. In any event, it appears, that the two criteria could be satisfied with wind tunnel experiments.

VII. References

1. G. E. Merritt, "Wake Growth and Collapse in Stratified Flow," AIAA Journal, Vol. 12 (7), pp. 940-949, July 1974.
2. R. J. Cresci, "Polytechnic Institute of New York - Environmental Wind Tunnel," J. Environ. Sys., Vol. 3 (3), pp. 233-251, Winter 1973.

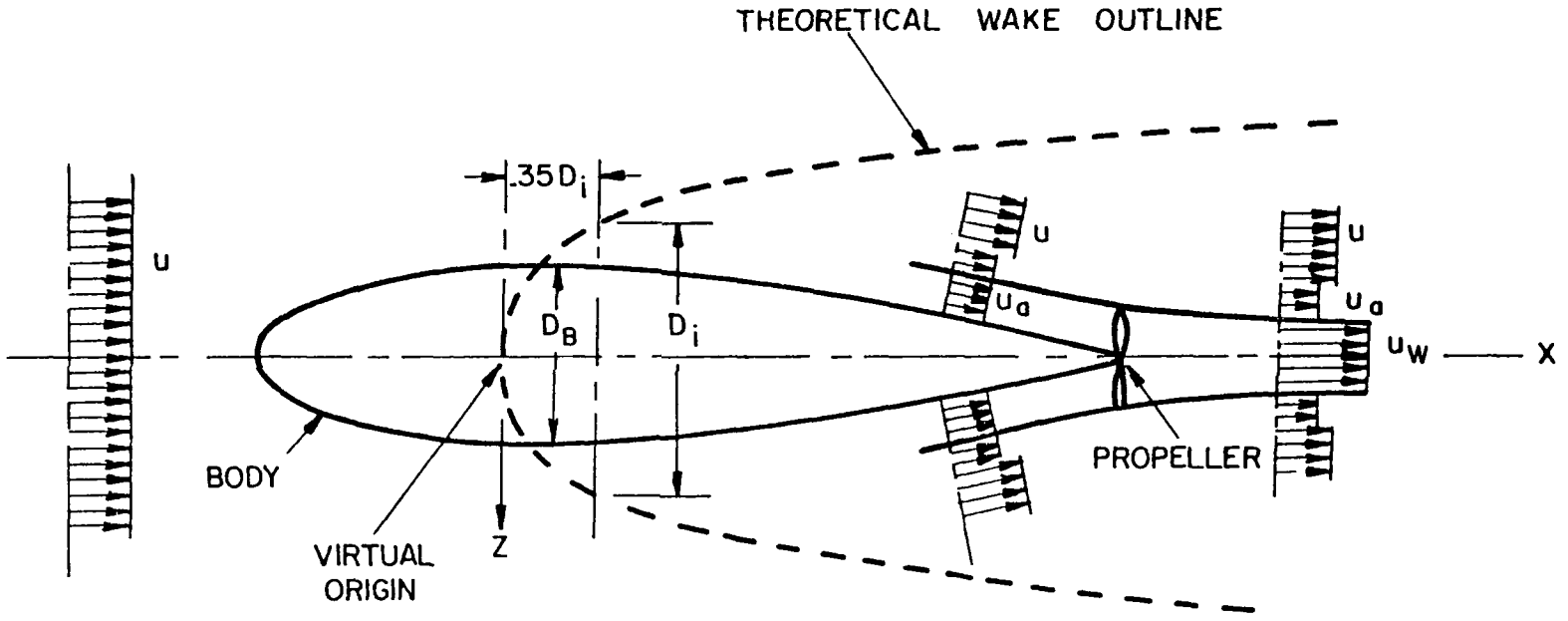

FIG. 1 FLOW FIELDS AROUND SUBMARINE BODY AND PROPELLER

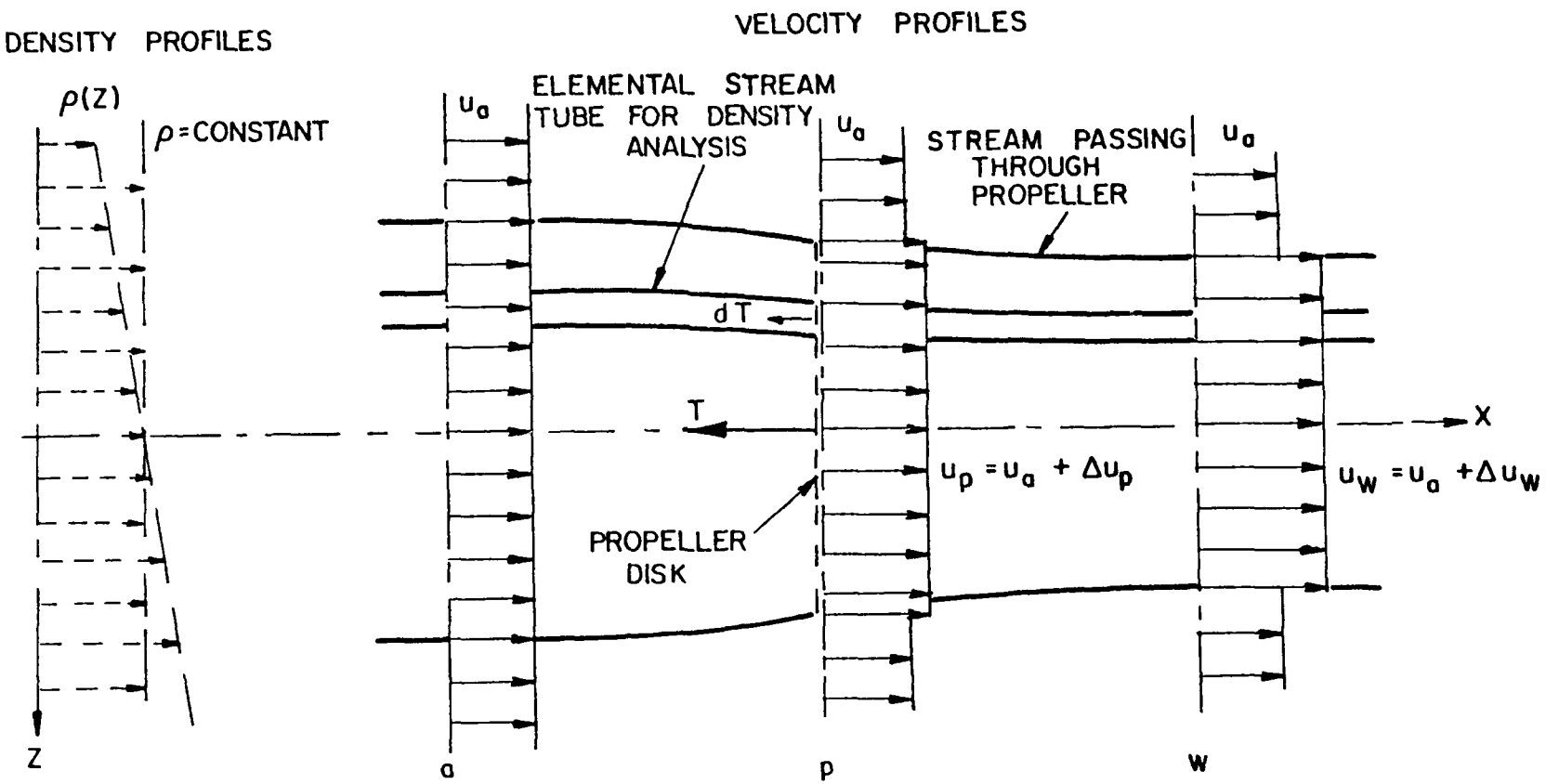

FIG. 2 PROPELLER FLOW FIELD FOR THE SIMPLE MOMENTUM THEORY

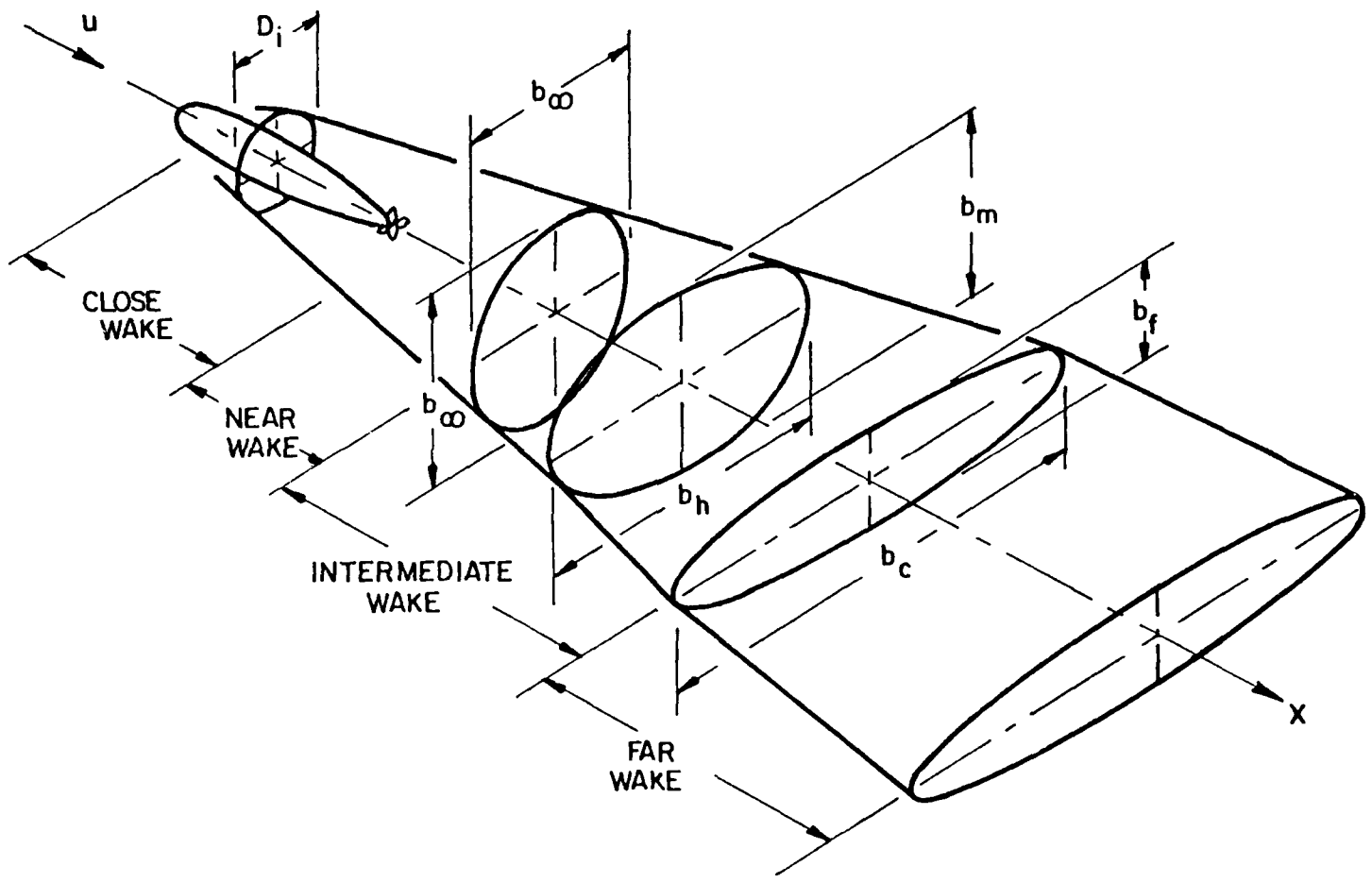

FIG. 3 WAKE DESIGNATIONS AND CROSS SECTIONS

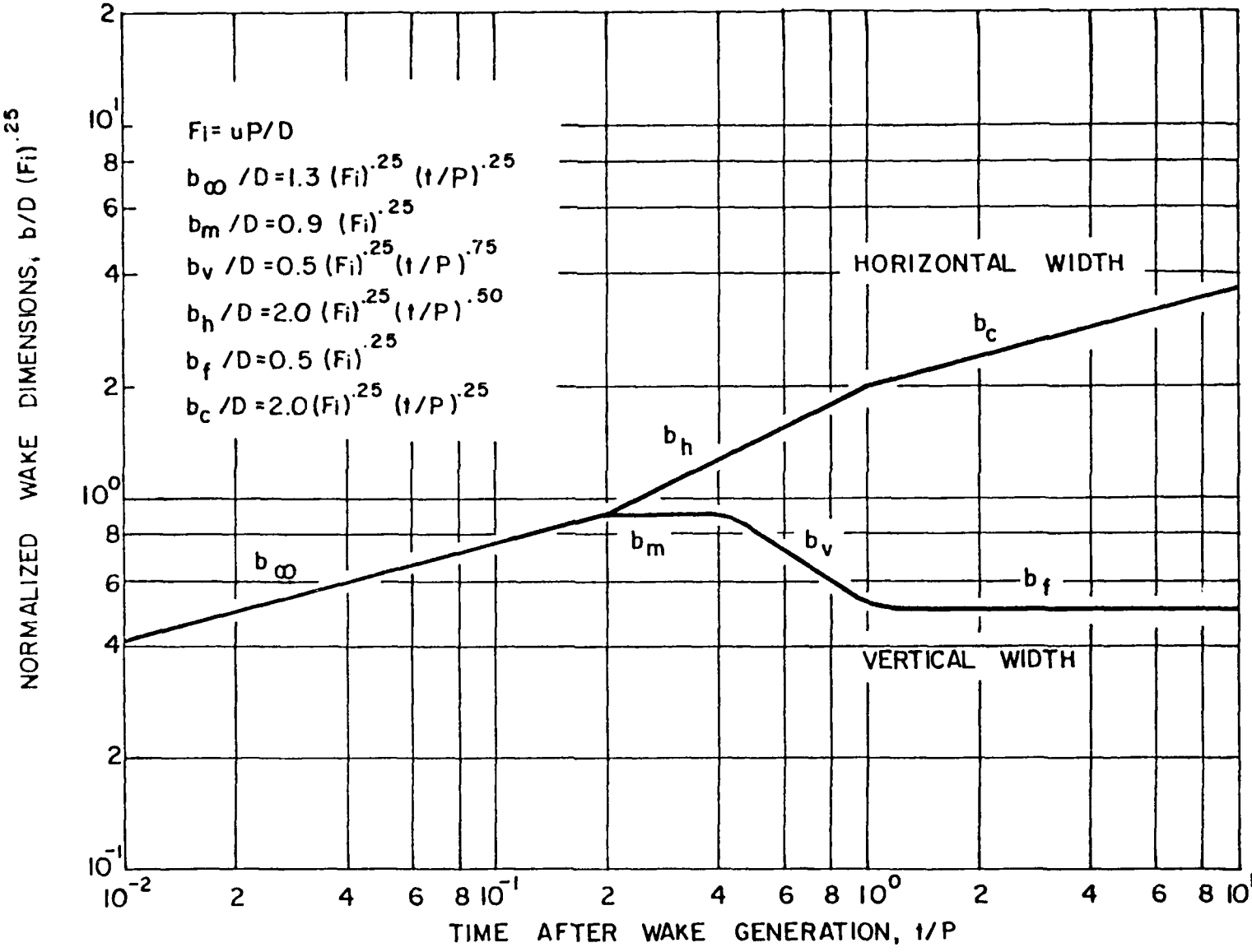

FIG. 4 WIDTHS AND HEIGHTS FOR WAKE EQUATIONS FROM MERRITT (REF. 1)

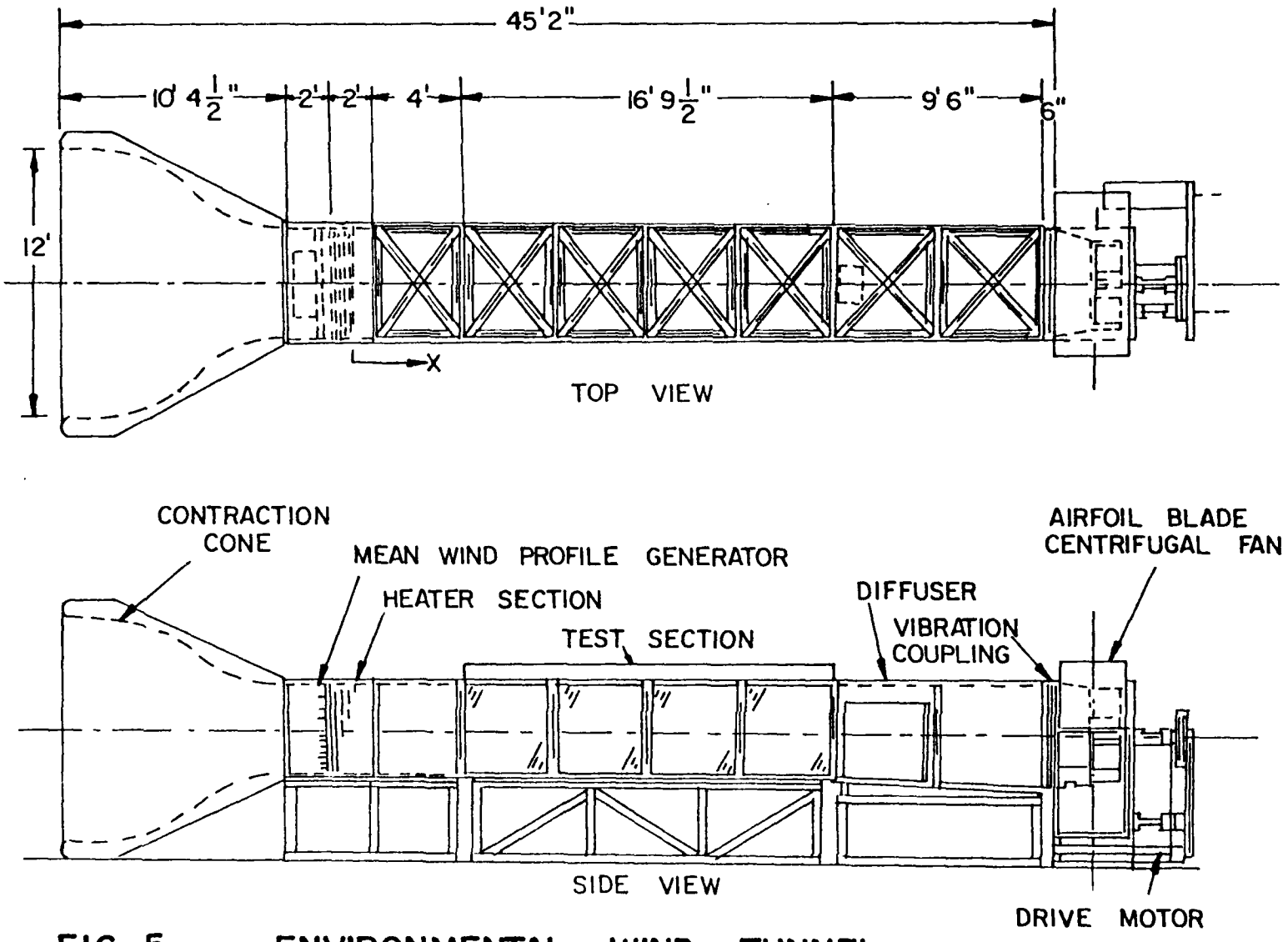

FIG. 5 ENVIRONMENTAL WIND TUNNEL

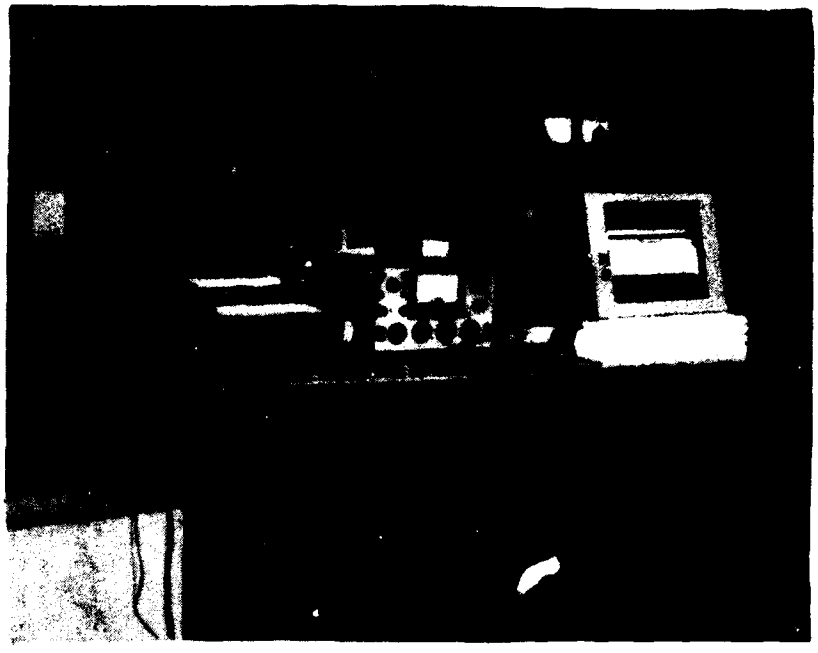

FIG. 6 VARIOUS INSTRUMENTS LOCATED ALONGSIDE THE TEST SECTION

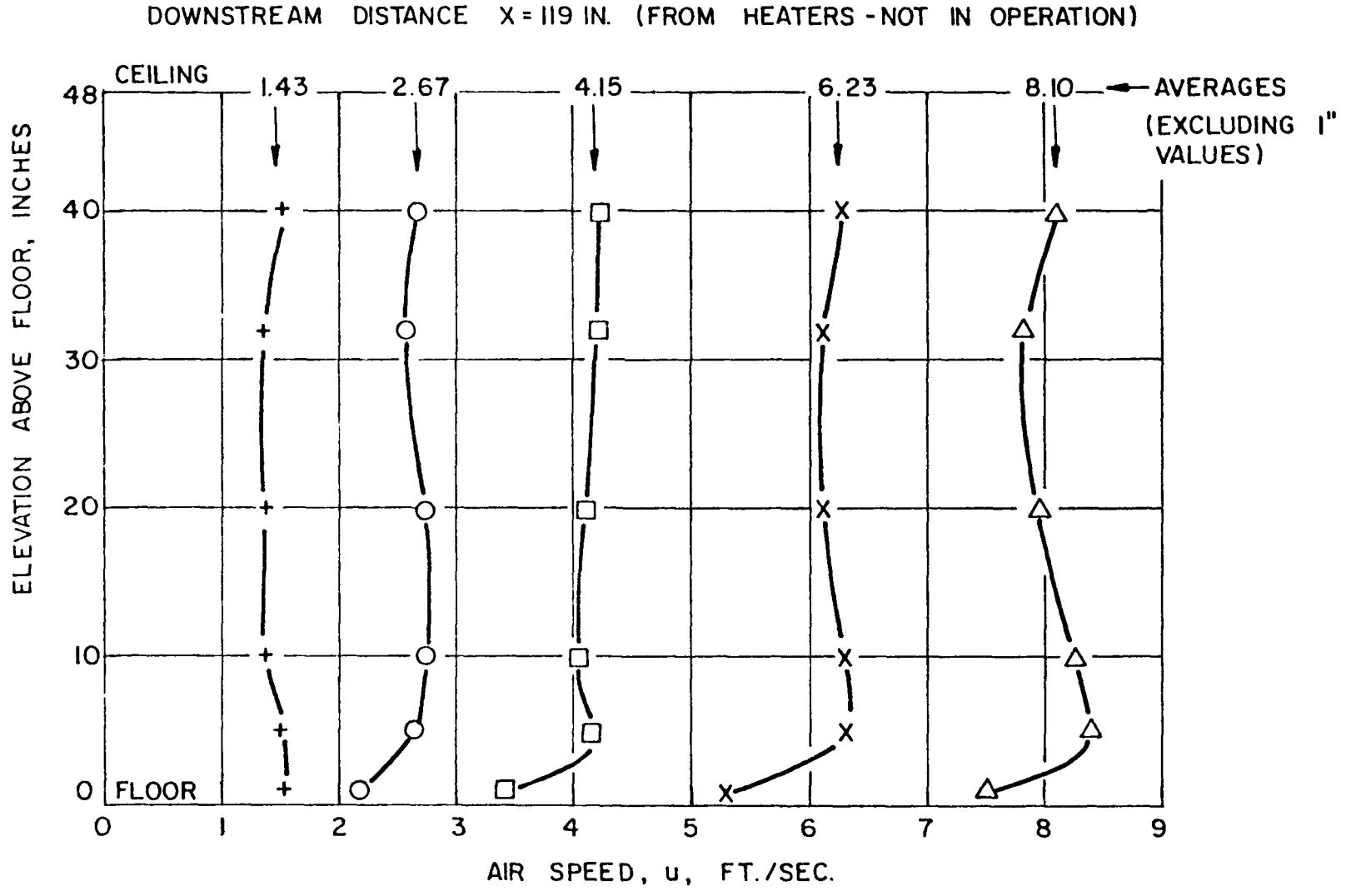

FIG. 7 AIR SPEED PROFILES

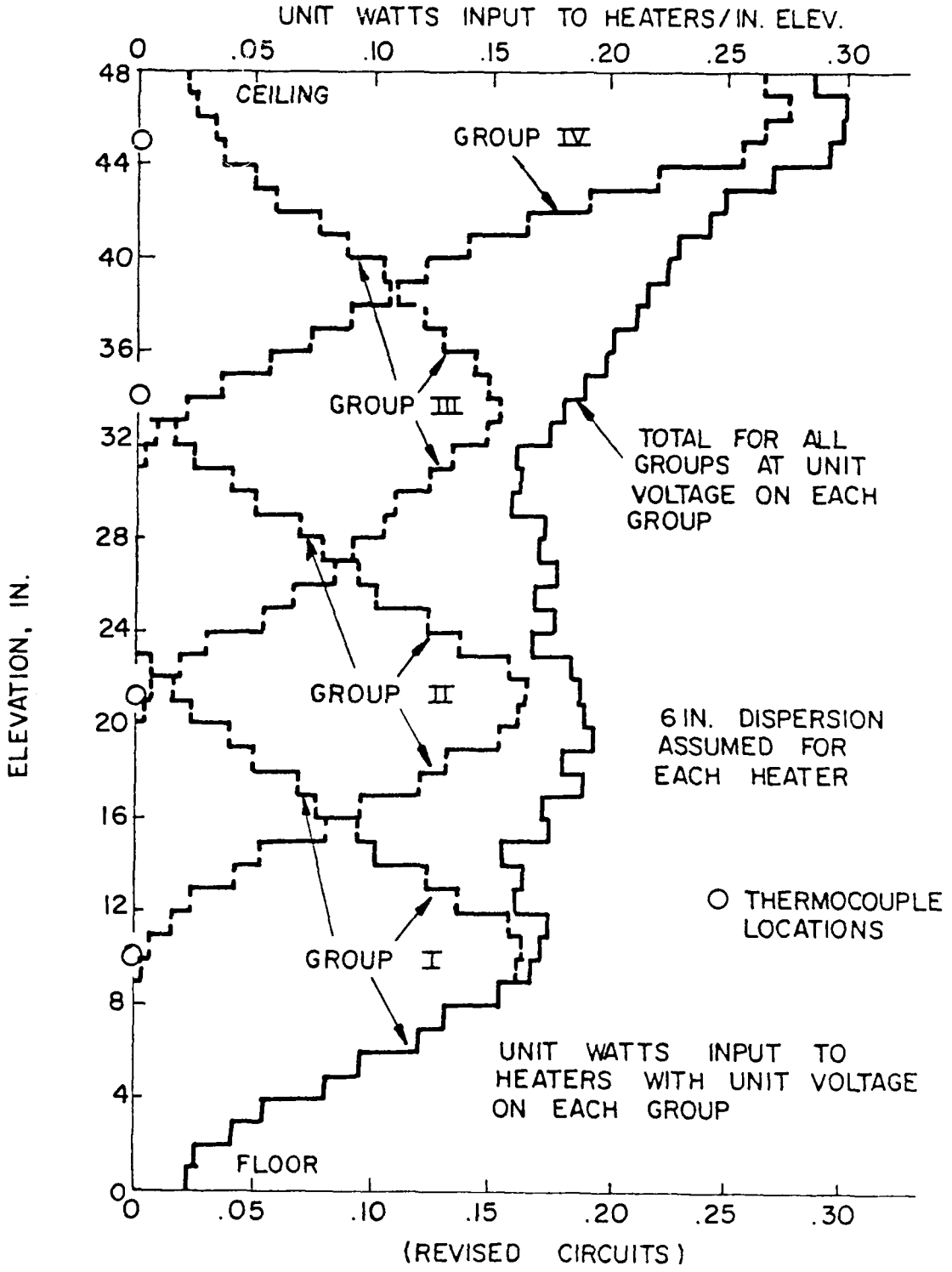

FIG. 8 CALCULATED HEAT INPUT PROFILES BY HEATER GROUPS

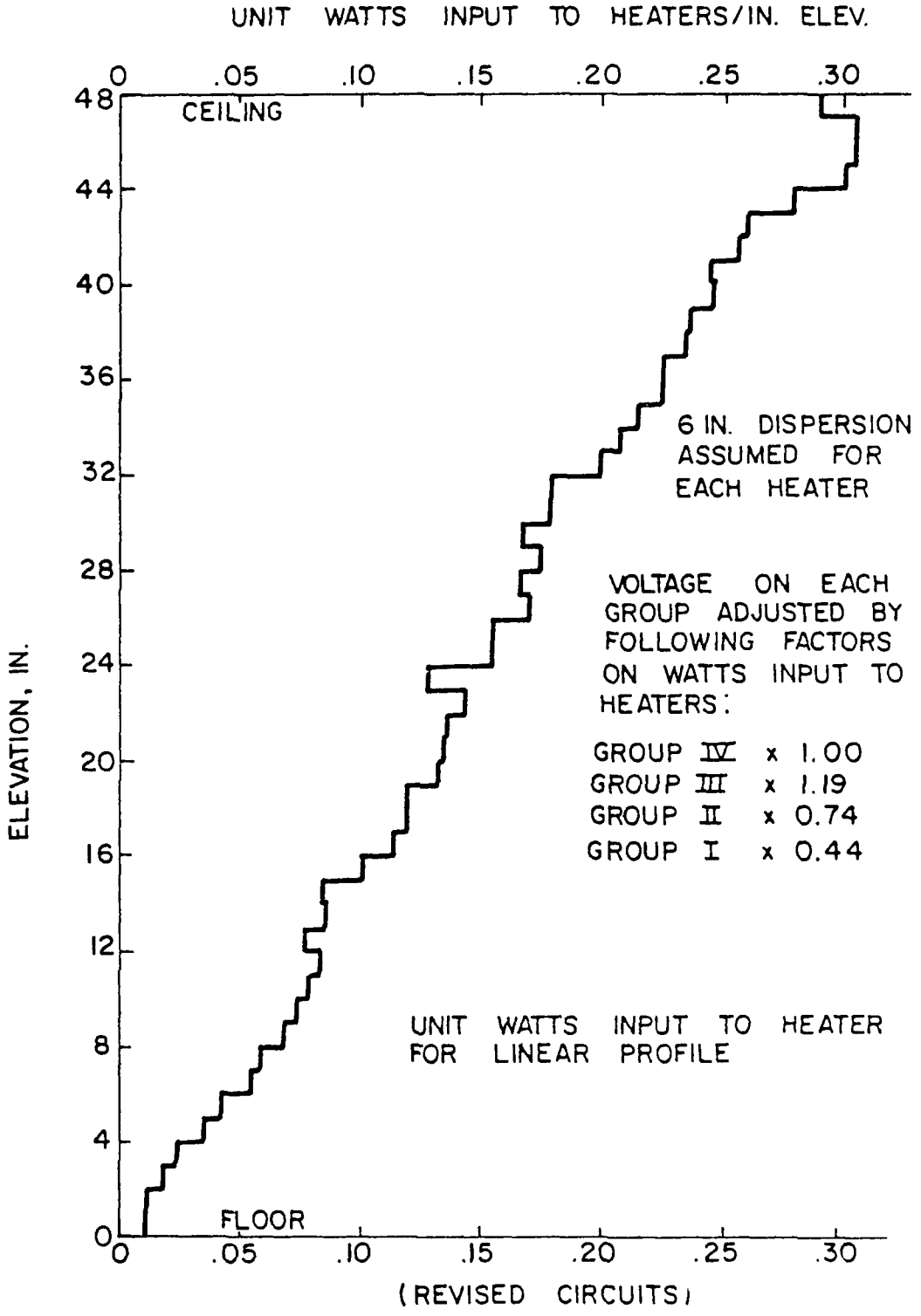

FIG. 9 CALCULATED HEAT INPUT PROFILES WITH ADJUSTED ELECTRIC INPUT

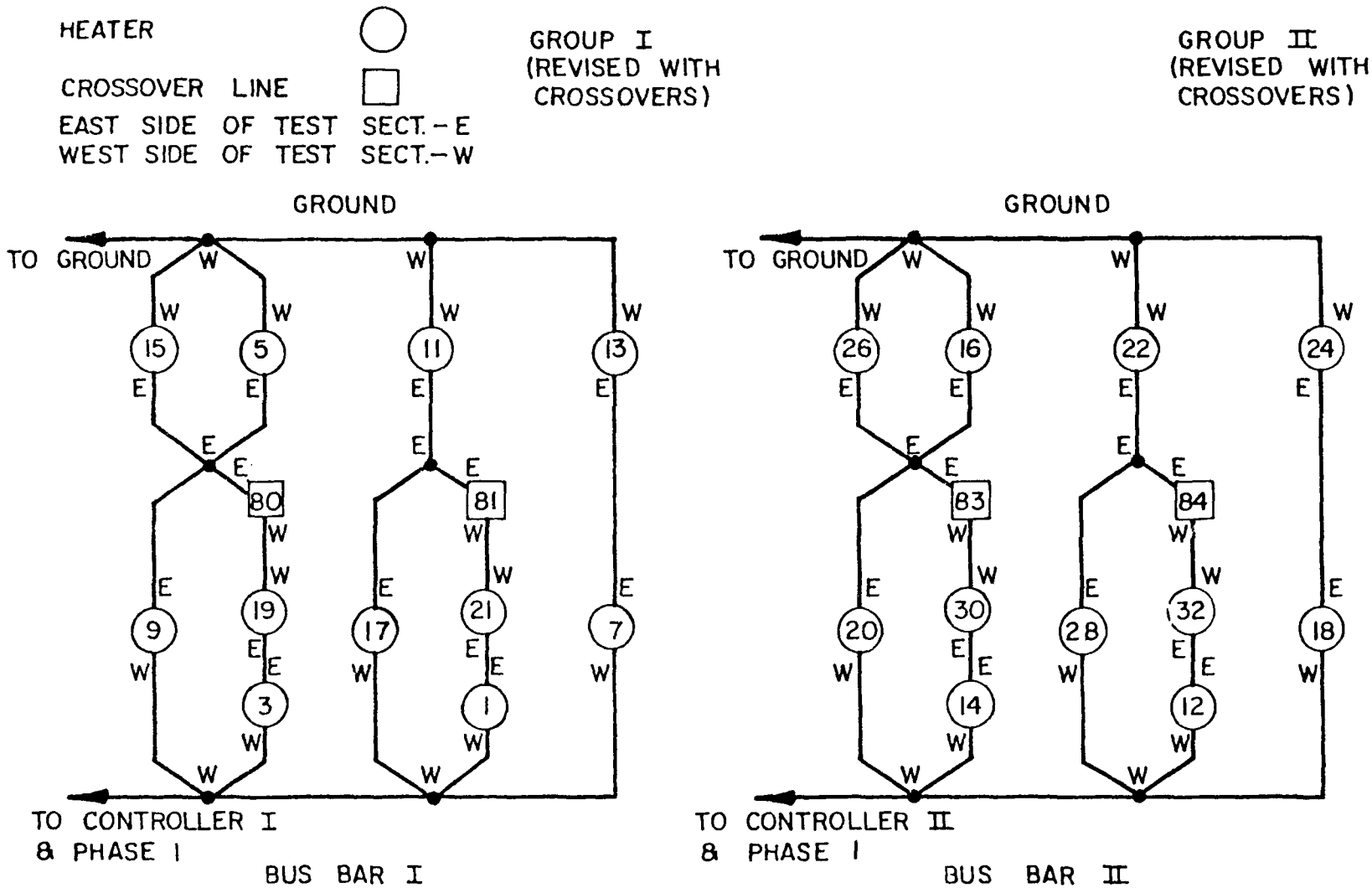

FIG. 10 a AIRSTREAM HEATER ELECTRIC CIRCUITS

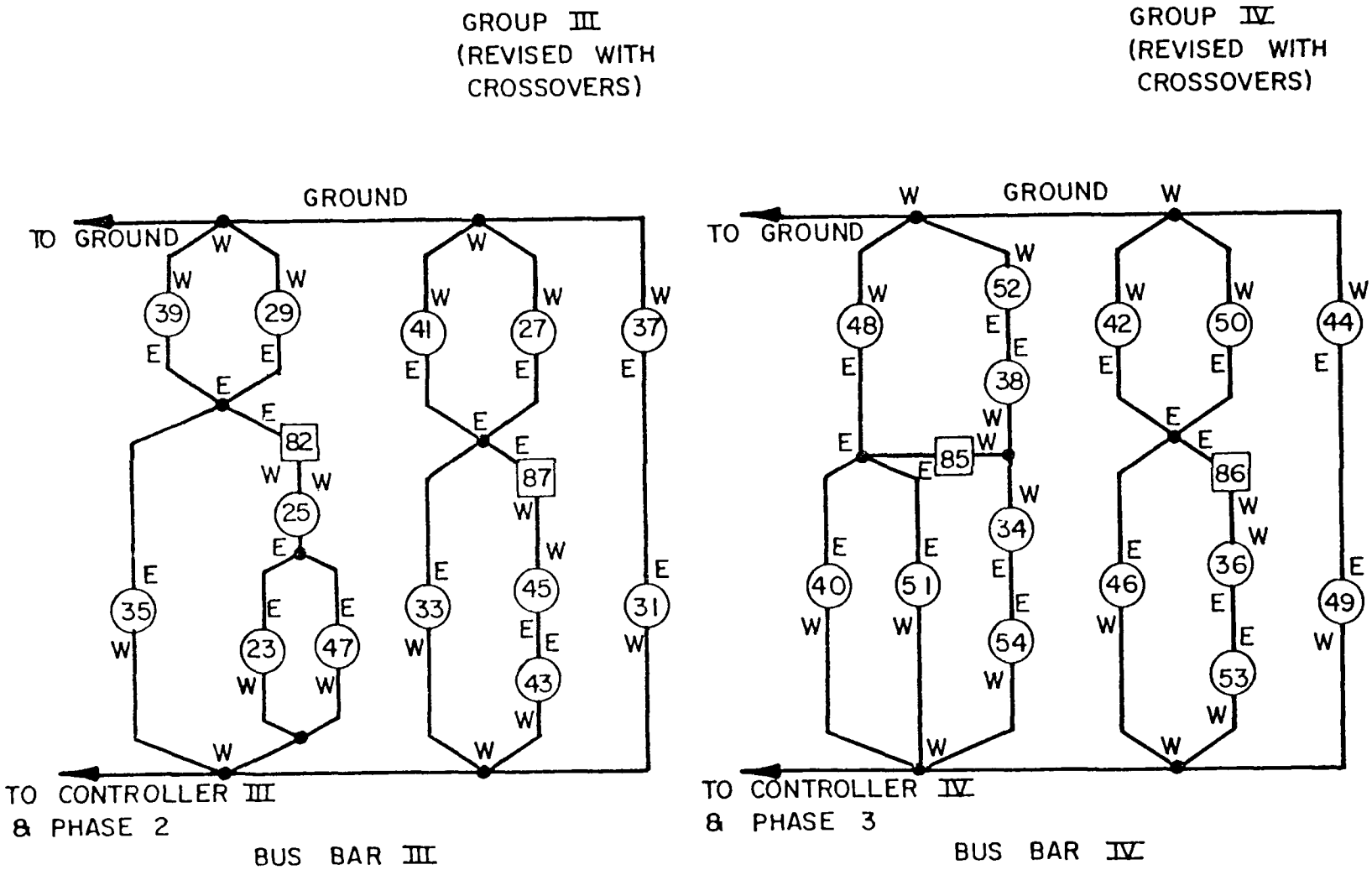

FIG. 10b AIRSTREAM HEATER ELECTRIC CIRCUITS

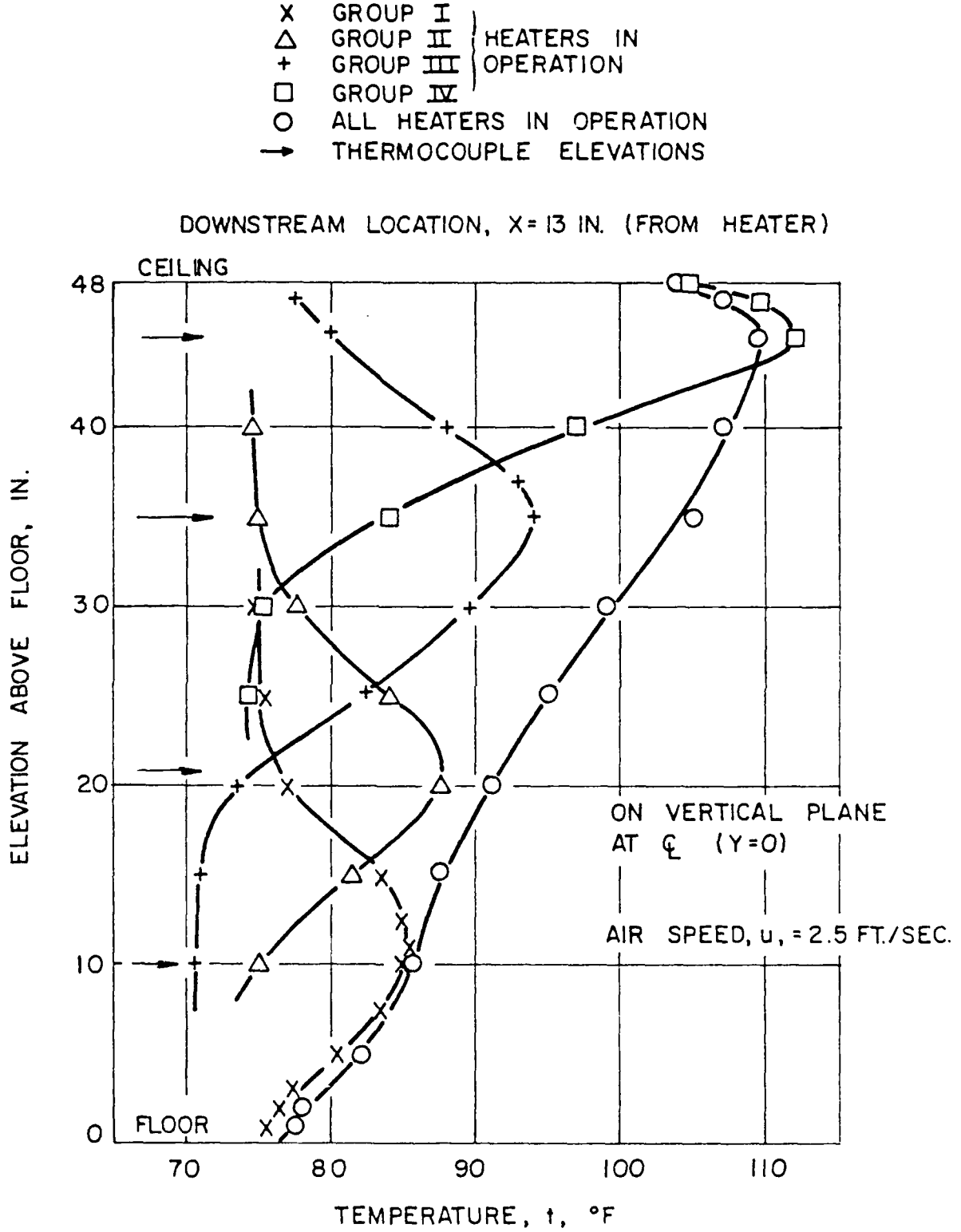

FIG. 11 TEMPERATURE PROFILES BY HEATER GROUP

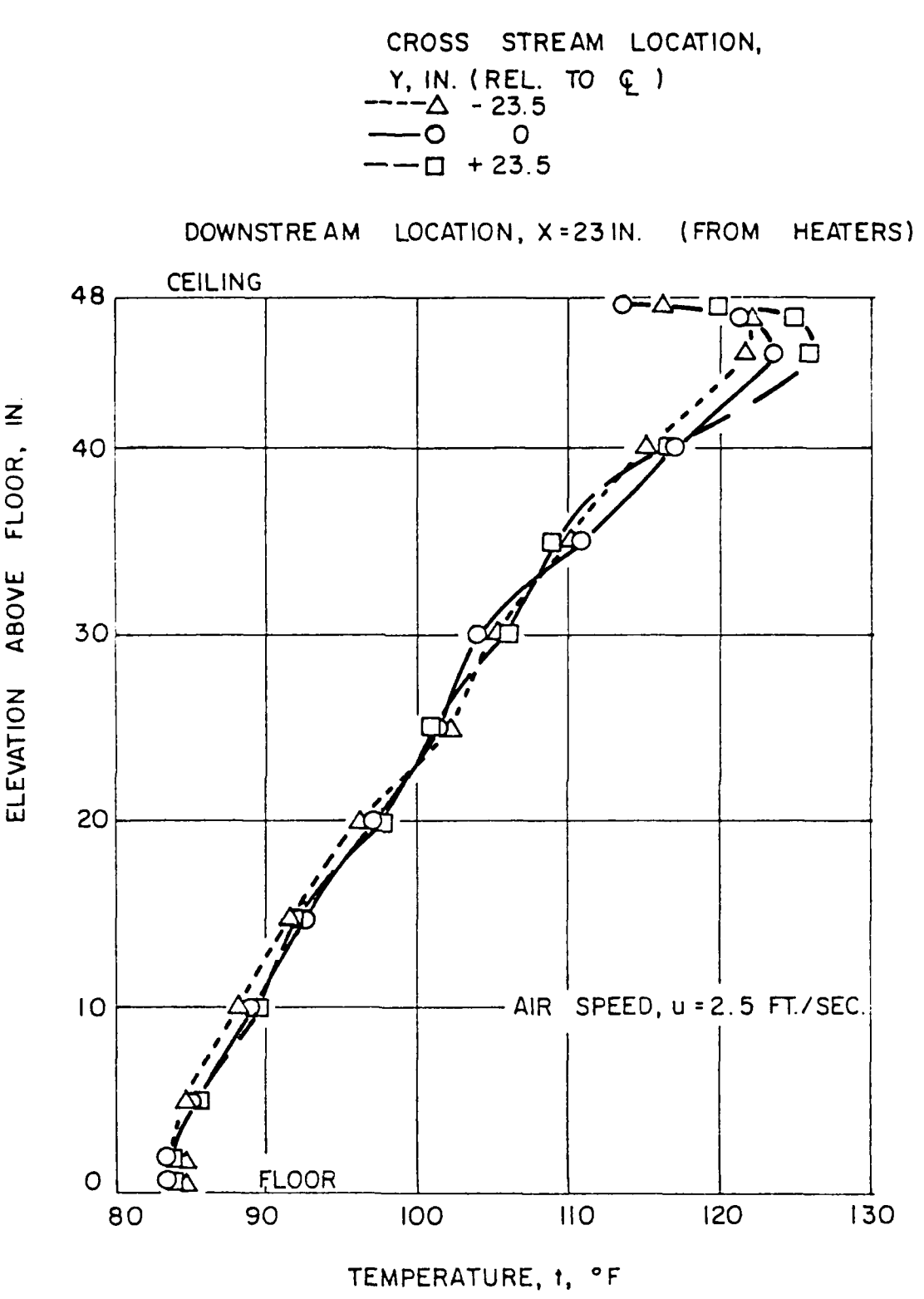

FIG. 12 TEMPERATURE PROFILES AT CROSS STREAM LOCATIONS

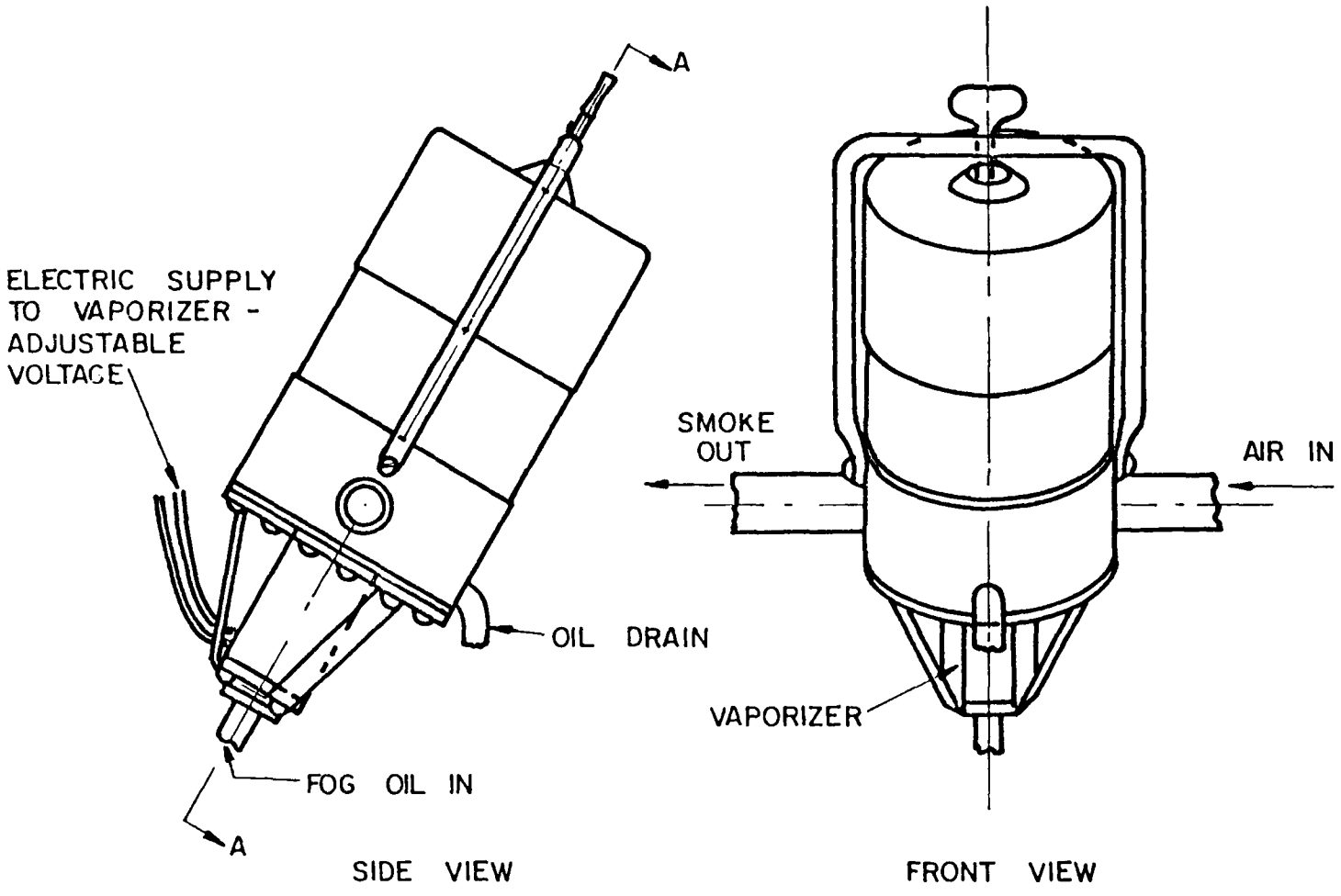

FIG. 13 SMOKE GENERATOR ASSEMBLY

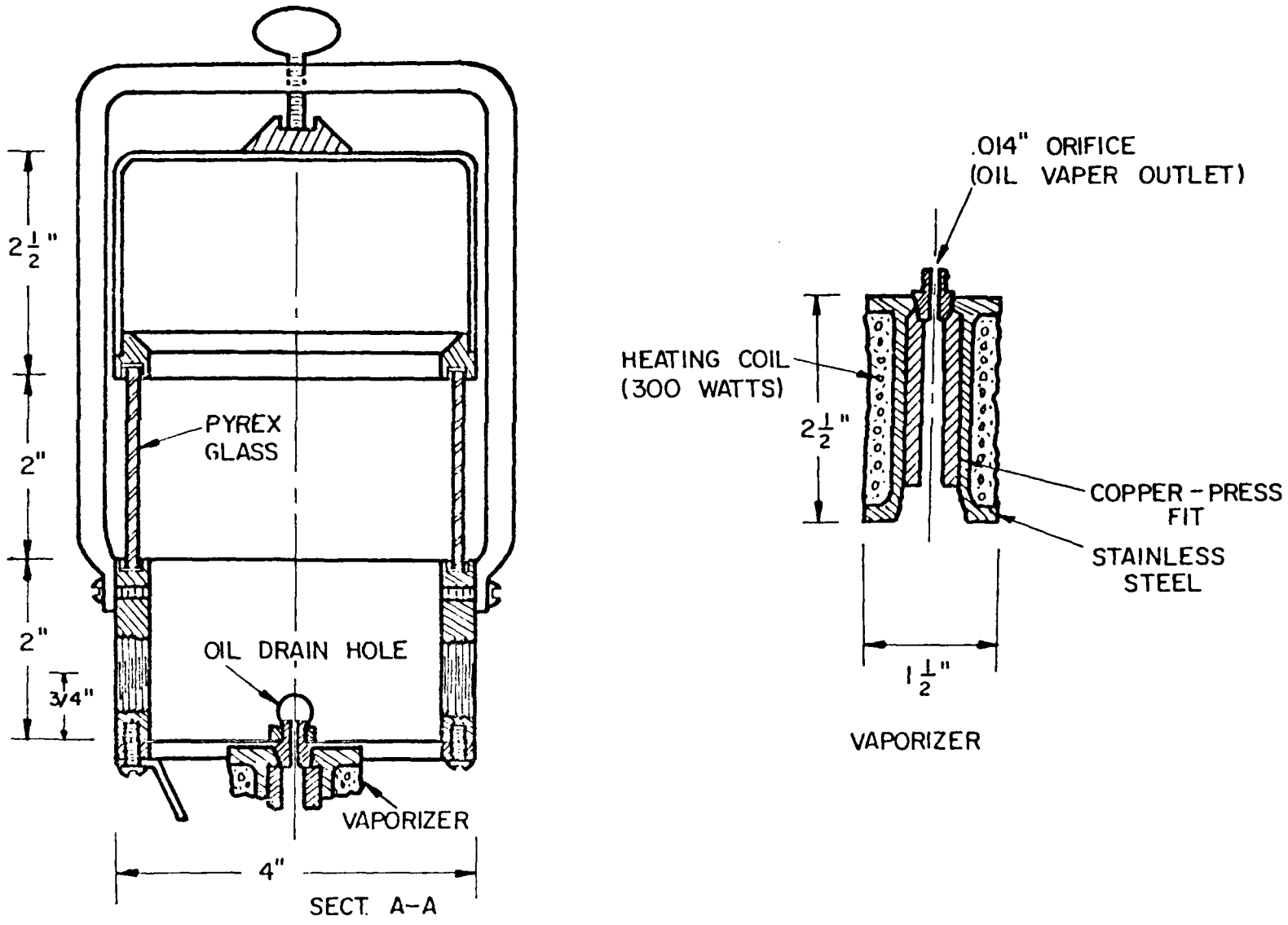

FIG. 14 SMOKE GENERATOR DETAILS

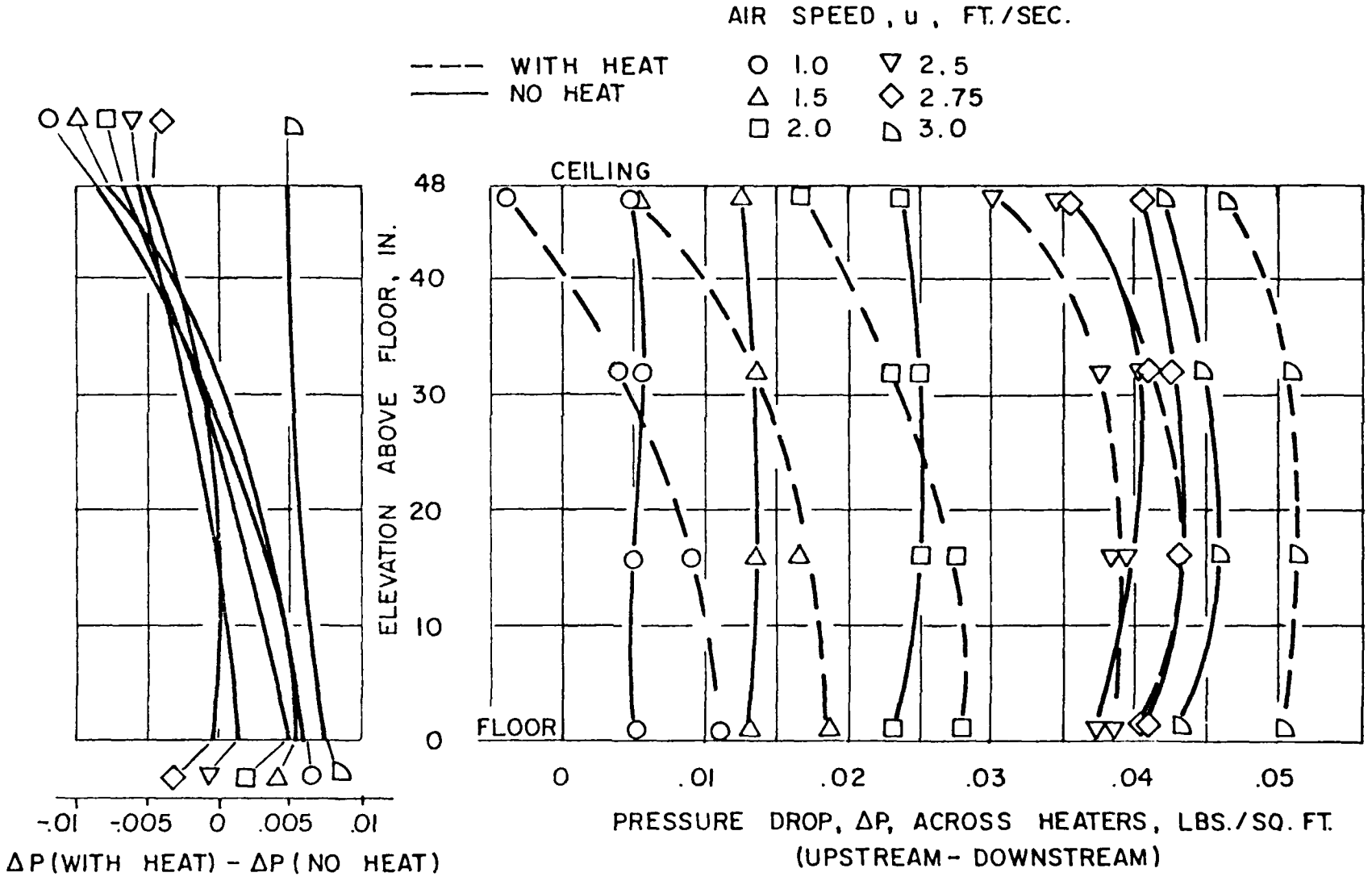

FIG. 15 PRESSURE DROP ACROSS HEATERS

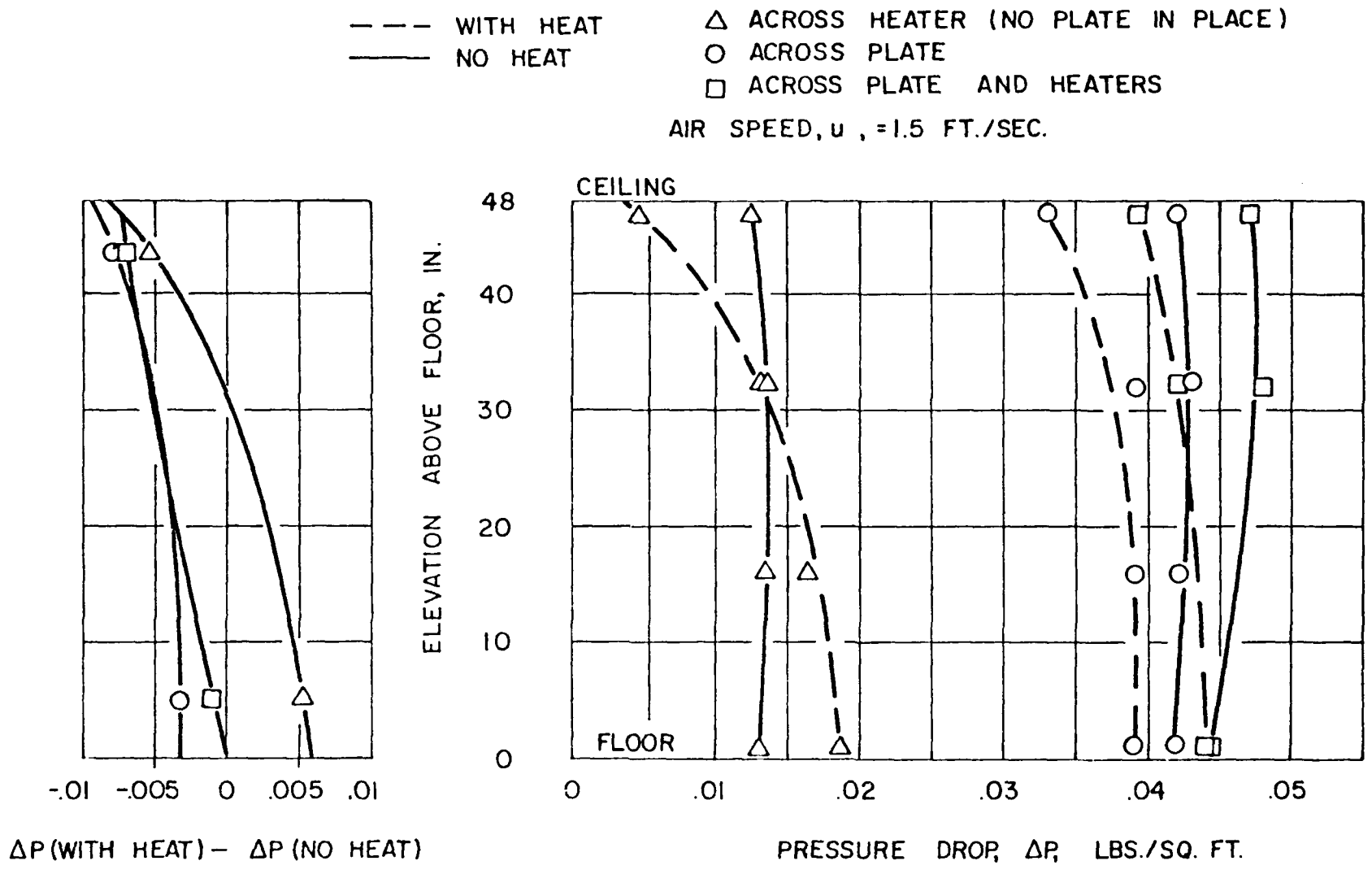

FIG. 16 PRESSURE DROP ACROSS EQUALIZER PLATE AND HEATERS

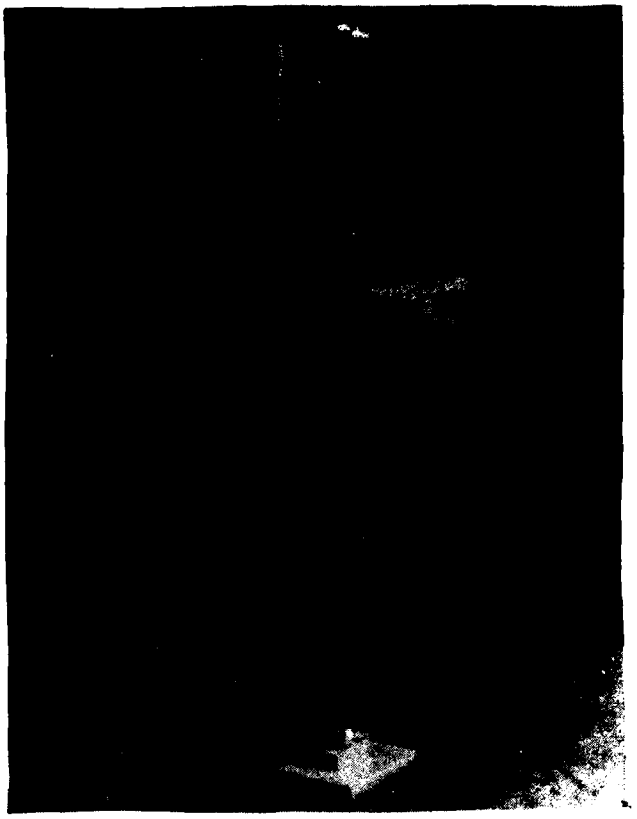

FIG. 17 SURVEY CARRIAGE

FIG. 18 PROPELLER ANEMOMETER

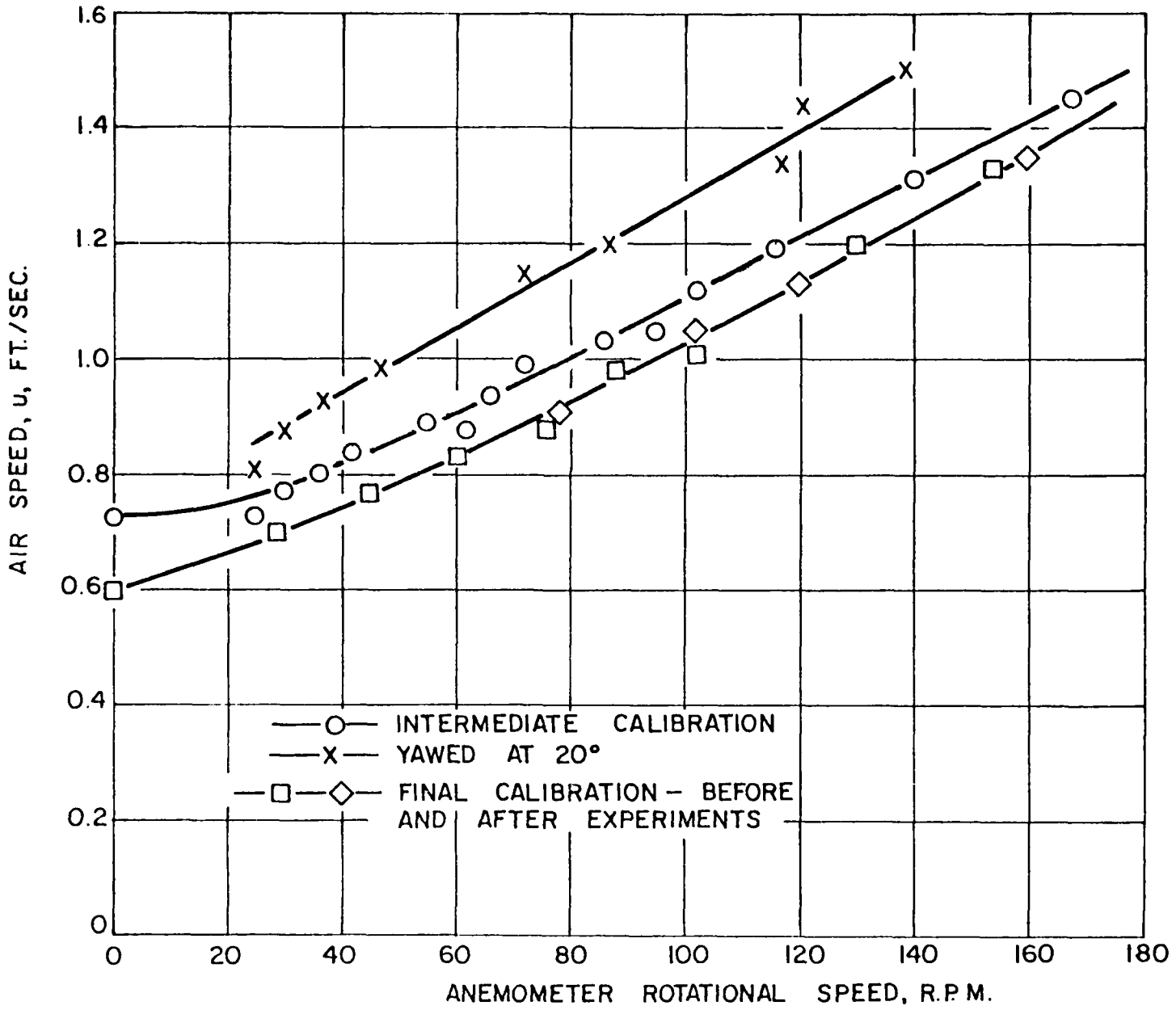

FIG. 19 PROPELLER ANEMOMETER CALIBRATION

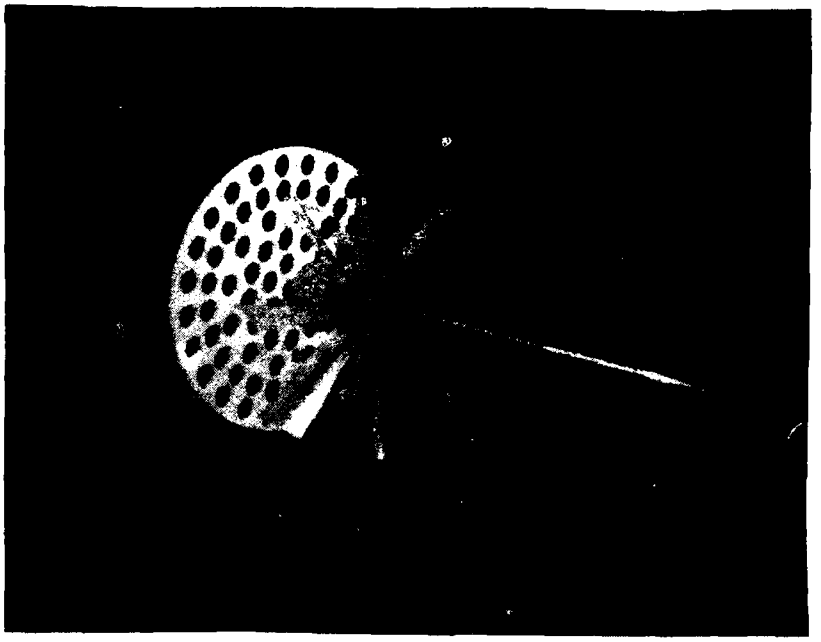

FIG. 20 DISK MODEL LOOKING FROM THE REAR

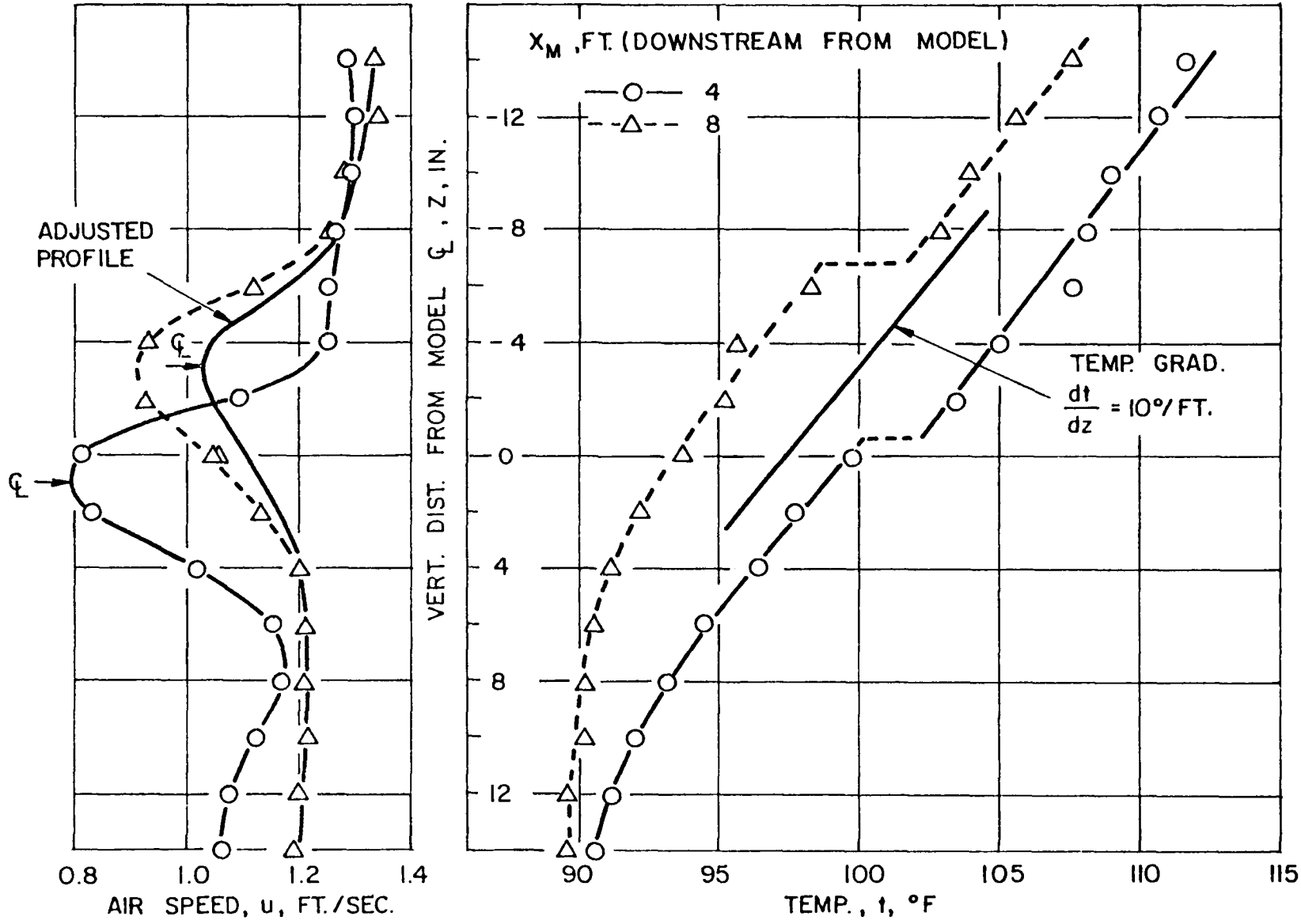

FIG. 21 VERTICAL WAKE AIR SPEED AND TEMPERATURE PROFILES – STRATIFIED FLOW

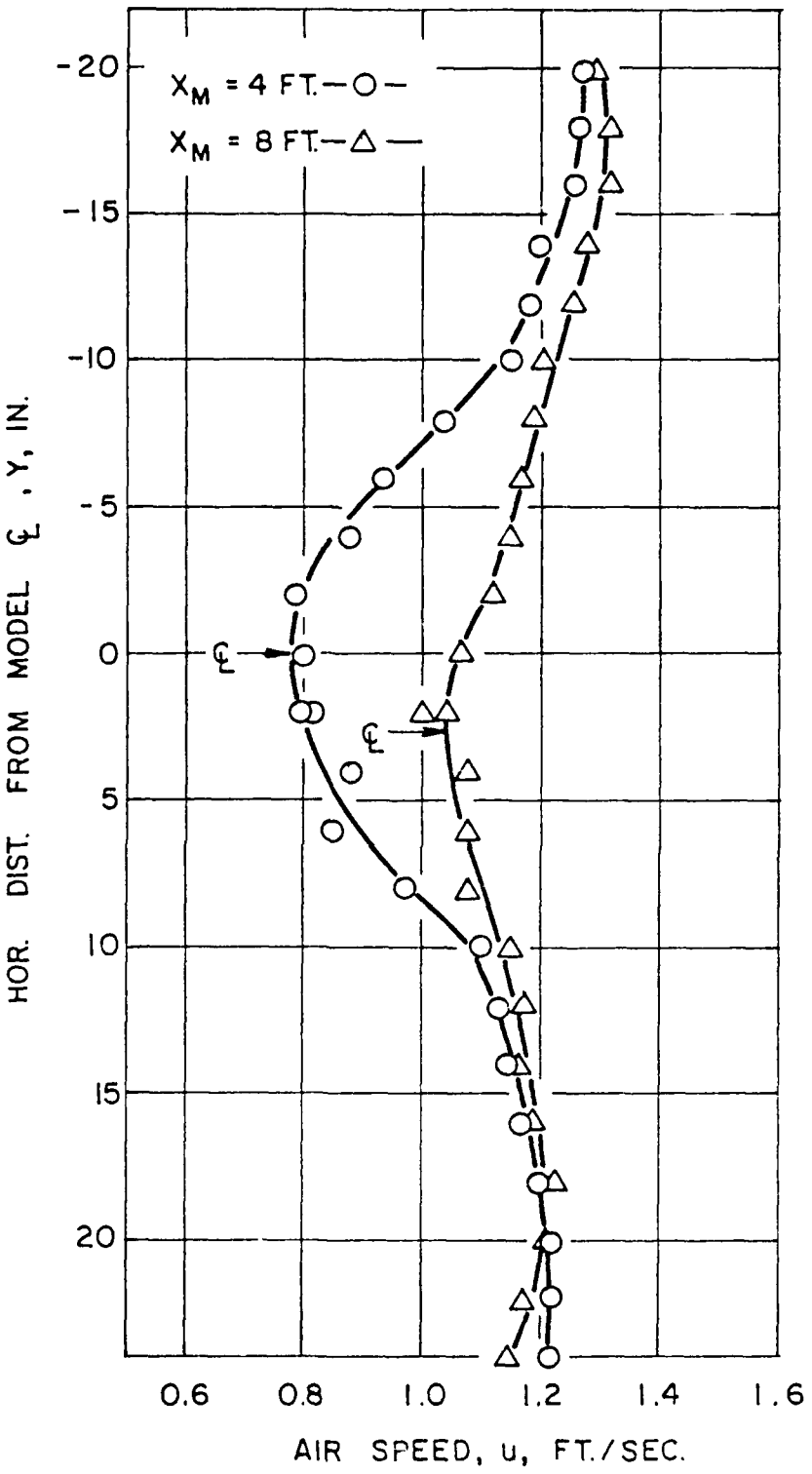

FIG. 22 HORIZONTAL WAKE AIR SPEED PROFILES - STRATIFIED FLOW

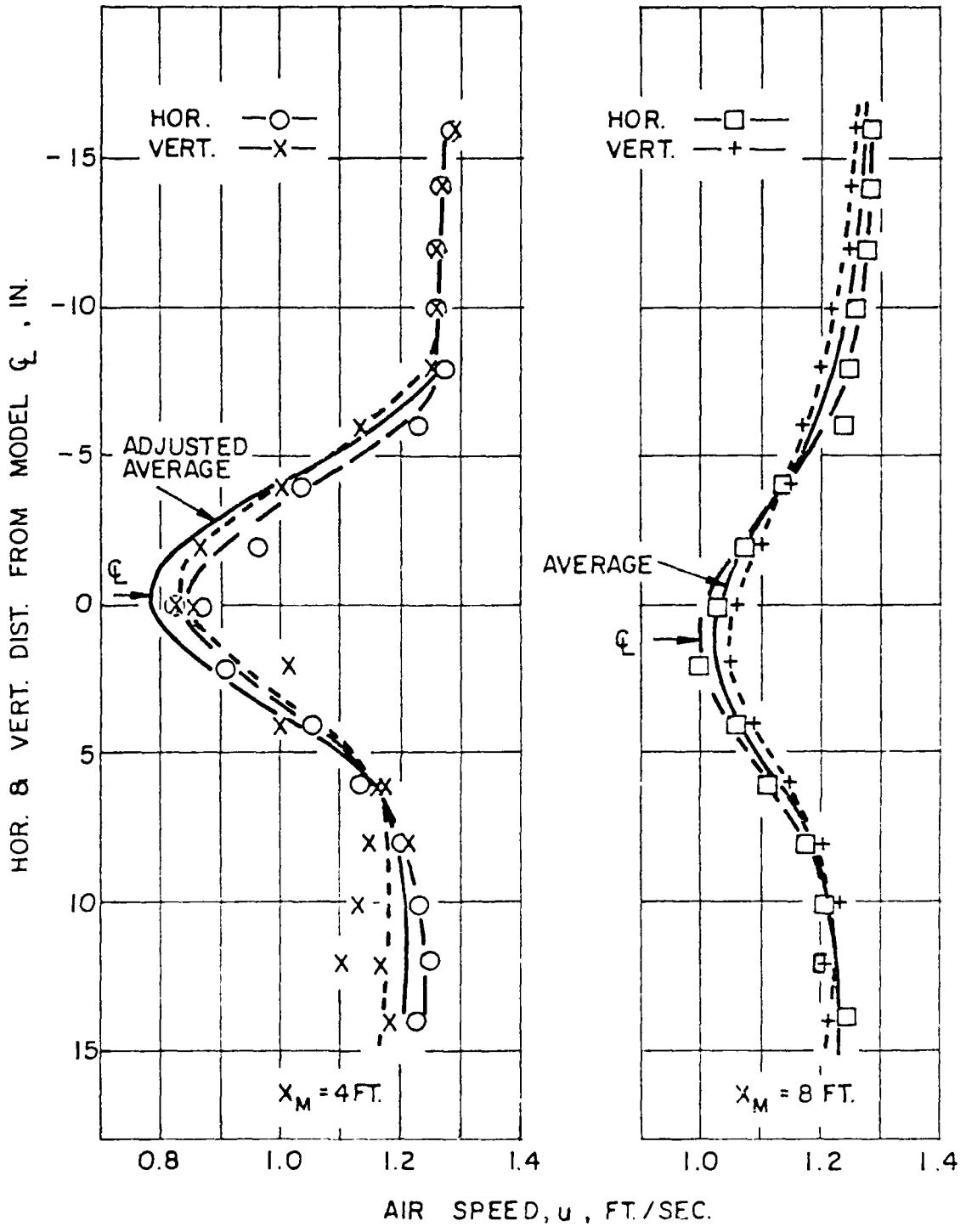

FIG. 23 HORIZONTAL AND VERTICAL WAKE AIR SPEED PROFILES - NEUTRAL TEMPERATURE GRADIENT

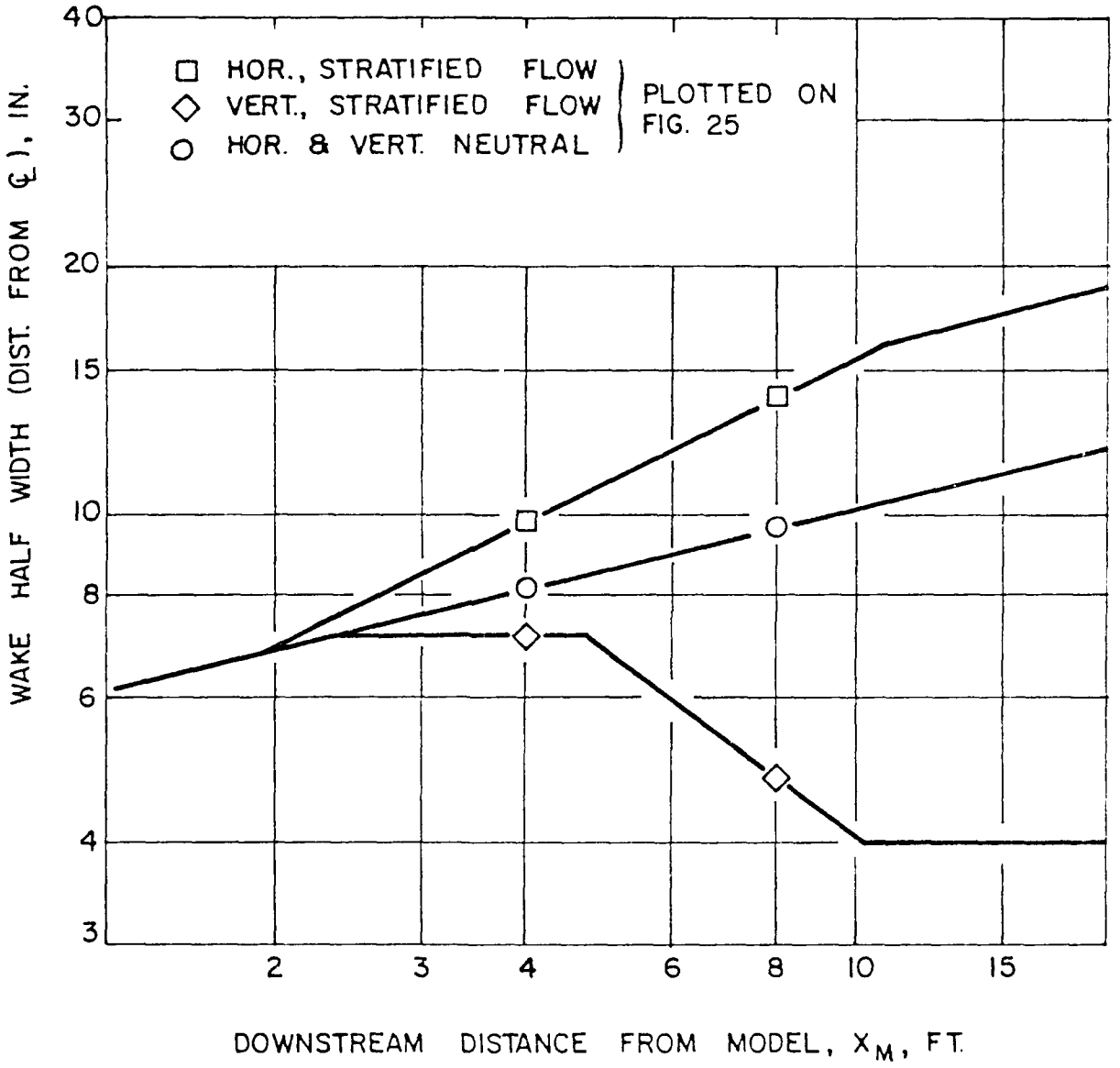

FIG. 24 MERRITT'S (REF 1) SCALING LAWS SPECIALIZED FOR THESE EXPERIMENTS

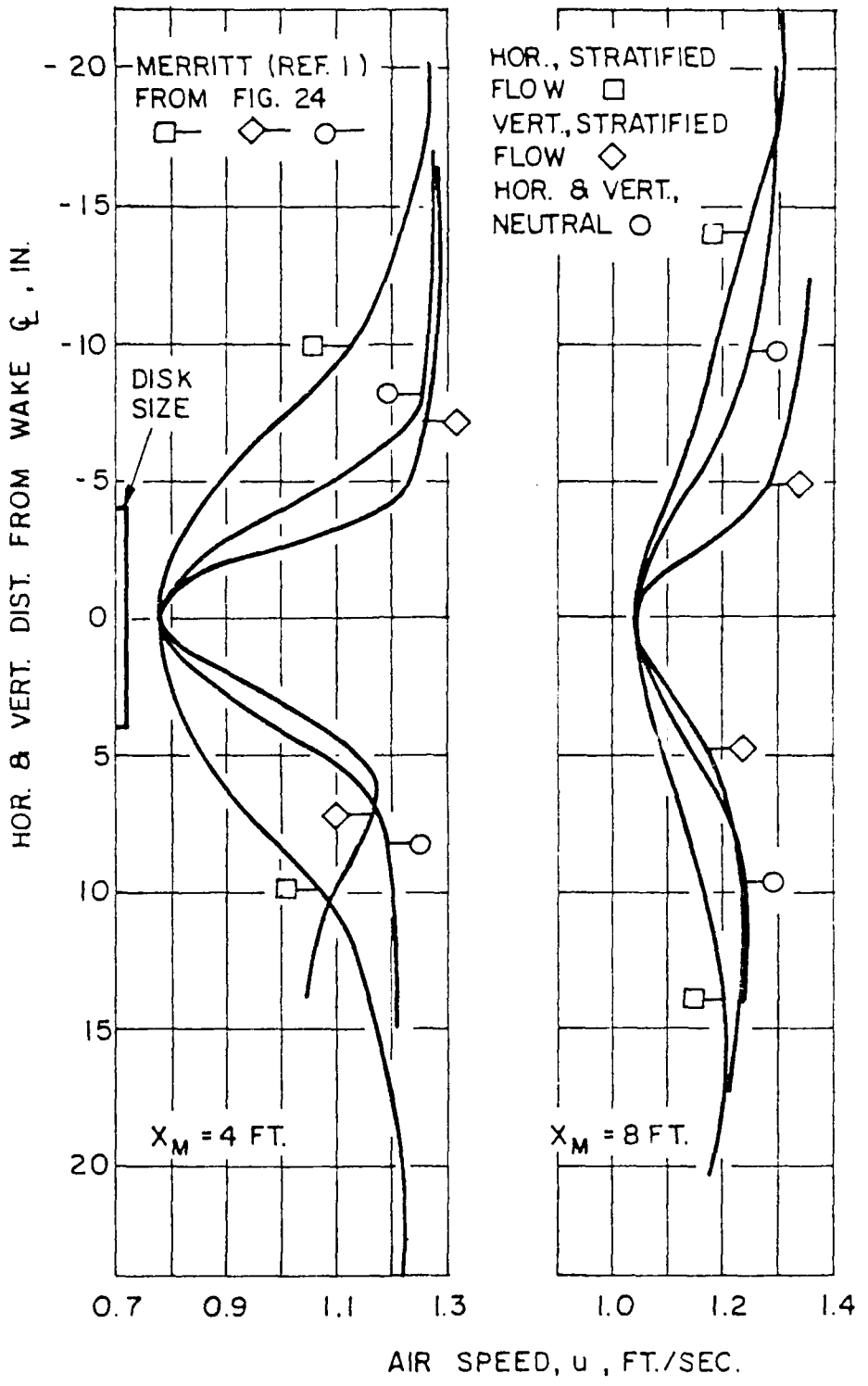

FIG. 25 WAKE AIR SPEED PROFILES - SUMMARY OF DATA

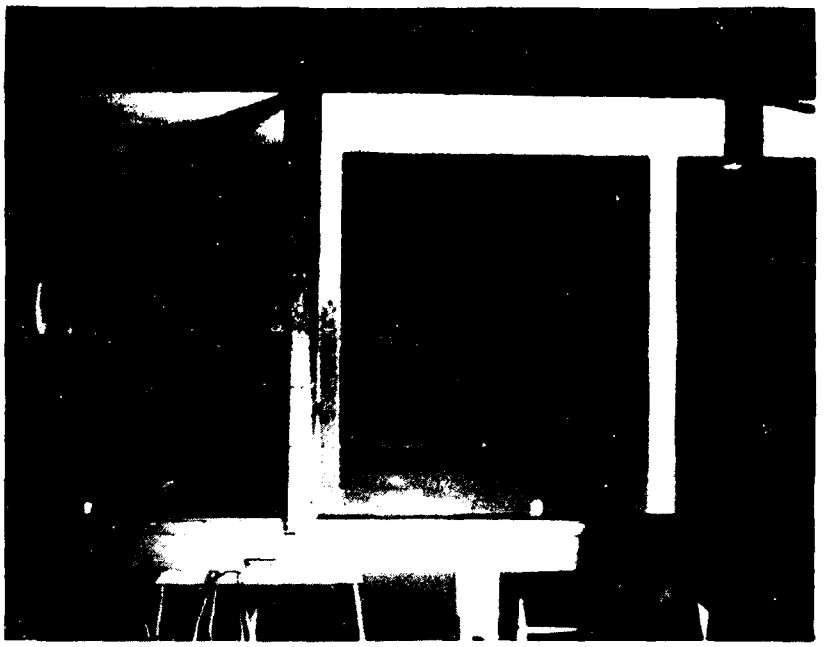

FIG. 26 SIDE VIEW OF WAKE-STRATIFIED FLOW - WITH SMOKE

FIG. 27 SIDE VIEW OF WAKE - NEUTRAL FLOW - WITH SMOKE

FIG. 28 WAKE LOOKING UPSTREAM-
STRATIFIED FLOW-WITH SMOKE

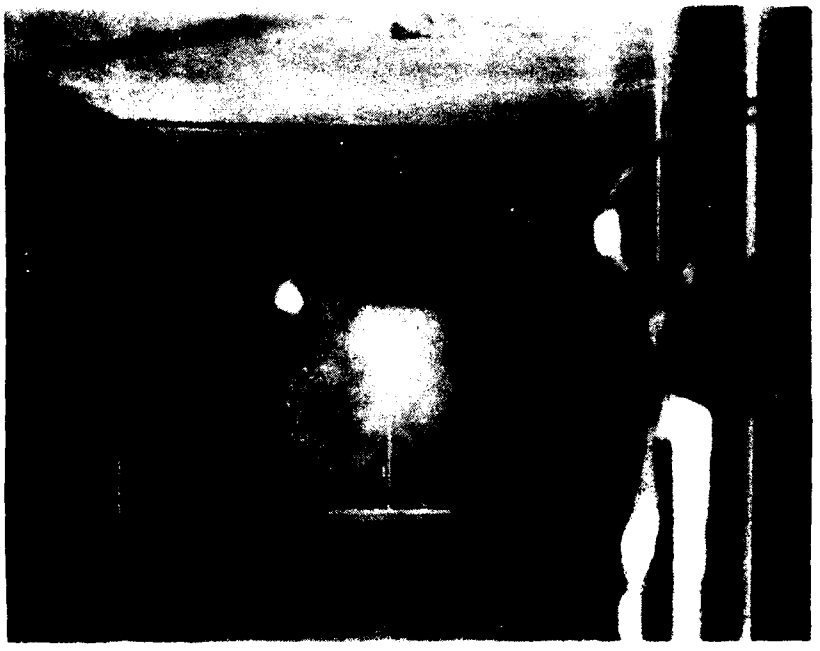

FIG. 29 WAKE LOOKING UPSTREAM -
NEUTRAL FLOW - WITH SMOKE